ELSEVIER

International Journal of Mass Spectrometry 219 (2002) 203–232

International Journal of Mass Spectrometry

www.elsevier.com/locate/ijms

Ab initio and MS/MS studies on protonated peptides containing basic and acidic amino acid residues I. Solvated proton vs. salt-bridged structures and the cleavage of the terminal amide bond of protonated RD-NH_2

Béla Paizs[a,*], Sándor Suhai[a], Balázs Hargittai[b,1], Victor J. Hruby[b], Árpád Somogyi[b]

[a] *Department of Molecular Biophysics, German Cancer Research Center, Im Neuenheimer Feld 280, D-69120 Heidelberg, Germany*
[b] *Department of Chemistry, University of Arizona, Tucson, AZ 85721, USA*

Received 12 July 2001; accepted 10 January 2002

Abstract

The results of a detailed ab initio investigation on one of the simplest model peptides, RD-NH_2, containing both basic (R) and acidic (D) residues are presented here. The ab initio (B3LYP/6-31+G(d,p)) relative energies of several internally solvated (IS) and salt-bridged (SB) structures are in the range of 0–33 kcal/mol. Upon ion activation in a tandem mass spectrometer, the conversion of IS into SB structures is energetically feasible but very probably kinetically controlled. Several theoretical pathways are suggested for the NH_3 loss from the amide terminus of protonated RD-NH_2. The loss of NH_3 is proposed to occur either via "four-center-one-step" (FCOS) processes or an "oxazolone ring" formation (OX). The FCOS pathways indicate that the formation of a SB structure is not a prerequisite for the loss of NH_3 from the amide terminus. The ab initio results clearly show the complexity of the potential energy surface of even such a small protonated peptide that is manifested in different protonated structures and pathways for a "simple" NH_3 loss. Low-energy CID MS^2 and MS^3 spectra of the singly charged RD-NH_2 have also been recorded and discussed in conjunction with the theoretical results. A brief discussion on the limitations of our current model to the fragmentation behavior of larger peptides containing both basic and acidic amino acids is also presented. (Int J Mass Spectrom 219 (2002) 203–232)

Keywords: Peptide fragmentation; Ab initio calculations; Tandem mass spectrometry; Proton transfer; Cleavage of amide bond

1. Introduction

The identification of a huge number of proteins and their mutants in cells of living organisms is one of the most important research projects. In these "proteomics" projects, which are currently performed in many laboratories all over the world, tandem mass spectrometry (MS/MS) is an important experimental method that allows rapid and reliable identification of proteins. The success of protein identification by MS/MS strongly depends on the number of fragments in the MS/MS spectra: fragment-rich spectra make sequencing more reliable. There are cases, however, when particular peptides exhibit poor MS/MS spectra, i.e., in which only a few fragment ions are detected. This is either due to specific and selective amide bond cleavages in peptides containing both basic (arginine,

* Corresponding author. E-mail: b.paizs@dkfz-heidelberg.de
[1] Present address: Department of Chemistry, Mathematics and Physical Sciences, St. Francis University, Loretto, PA 15940, USA.

1387-3806/02/$ – see front matter
PII S1387-3806(02)00560-2

R, lysine, K, and histidine, H) and acidic residues (cysteic acid, C*, aspartic acid, D, and glutamic acid, E) [1–7] or the lack of amide bond dissociation (of those, e.g., that are neighboring to proline, P [8]). The better understanding of these "selective fragmentation" mechanisms could certainly lead to the further improvement of the "mobile proton" model [5–17] which is now widely accepted for the description of the main features of peptide fragmentation. The incorporation of these "experimental rules" to automated peptide sequencing programs (such as SEQUEST [18]) can also be a challenging goal in future [6].

The present work is the first part of a collaborative project devoted to the theoretical and experimental investigation of specific and selective fragmentation pathways of protonated peptides containing both basic and acidic amino acid residues. Our strategy is based on intensive interplay between theoretical (such as high level of ab initio calculations) and experimental (tandem mass spectrometry, MS/MS) tools to find out the most important energetic and mechanistic features of fragmentation of these protonated peptides.

This work has been directly inspired by numerous papers [1–7] that have appeared in the literature on peptides containing both basic and acidic amino acids (AAs). Selective fragmentation at acidic residues is of great importance in those cases when trypsin is used to digest the proteins investigated. Because tryptic peptides always contain basic amino acids (lysine or arginine), acid–base interactions frequently play a role in the structure and, therefore, the fragmentation of such protonated peptides.

Because the side-chains of K and R contain functionalities of high proton affinities (PAs), it can be assumed that these groups are nearly always protonated under the most common experimental (such as electrospray ionization, ESI) conditions. Therefore, the most important structure determining factor is "*internal solvation*" (IS) of the protonated K or R side-chains by various electron-rich groups of the rest of the molecule. Carboxylic groups in side-chains of acidic residues, the terminal amino group, and the amide oxygen function as electron-donors; their role is simply solvation of the protonated basic moiety of the ion by H-bonding. Upon ion activation, there is a competition between the electron-rich groups of the molecule which results in large numbers of possible conformers in a wide range of energy. If the acid–base interaction is strong enough, formation of a *salt-bridge* (or, in other words, protonated zwitterion, see below) can take place [1,4,5] with a simultaneous transfer of the acidic proton of the acidic side-chain to other functional groups of the molecule. The nature of these interactions depends on the amino acids involved, size of the peptide, internal energy of the ions formed, etc. The presence of a salt-bridge can have a pronounced effect on the fragmentation of protonated and/or alkylated [19] peptides, as well as on the stability of amino acid aggregates [20].

Yu et al. [1] have investigated the origin of facile cleavages at Asp–Pro and Asp–Xxx peptide bonds by MALDI-TOF mass spectrometry (Xxx denotes other amino acids). They have found that the Asp–Pro peptide bond is more labile than the other peptide bonds independent of the size of the peptide investigated. The key role of the aspartic acid side-chain in the lability of the Asp–Pro peptide bond has been demonstrated by esterification in the same study. The mechanism proposed to account for this selective and facile cleavage is shown in Scheme 1a (Path A, compiled for the case of protonated RD-NH_2). As can be seen in Scheme 1a, it is assumed that the "ionizing" proton added to the system is sequestered by the arginine (basic) side-chain. In the first step, the acidic proton of COOH transfers to the nitrogen of the amide bond adjacent to the aspartic acid (D) residue. Due to the excess energy deposited on the ion during its formation and excitation, the Asp–Xxx bond cleaves forming a cyclic anhydride and NH_3. Bakhtiar et al. [2] have proved that the above Asp-effect is charge specific. They have found that cleavage of the Asp(75)–Met(76) peptide bond in the α-chain of human apohemoglobin is observed primarily in the +11 and +12 ionization states of the protein. Quin and Chait [3] have also observed preferential cleavage of the peptide bonds adjacent to Asp and Glu residues using a MALDI ion trap mass spectrometer.

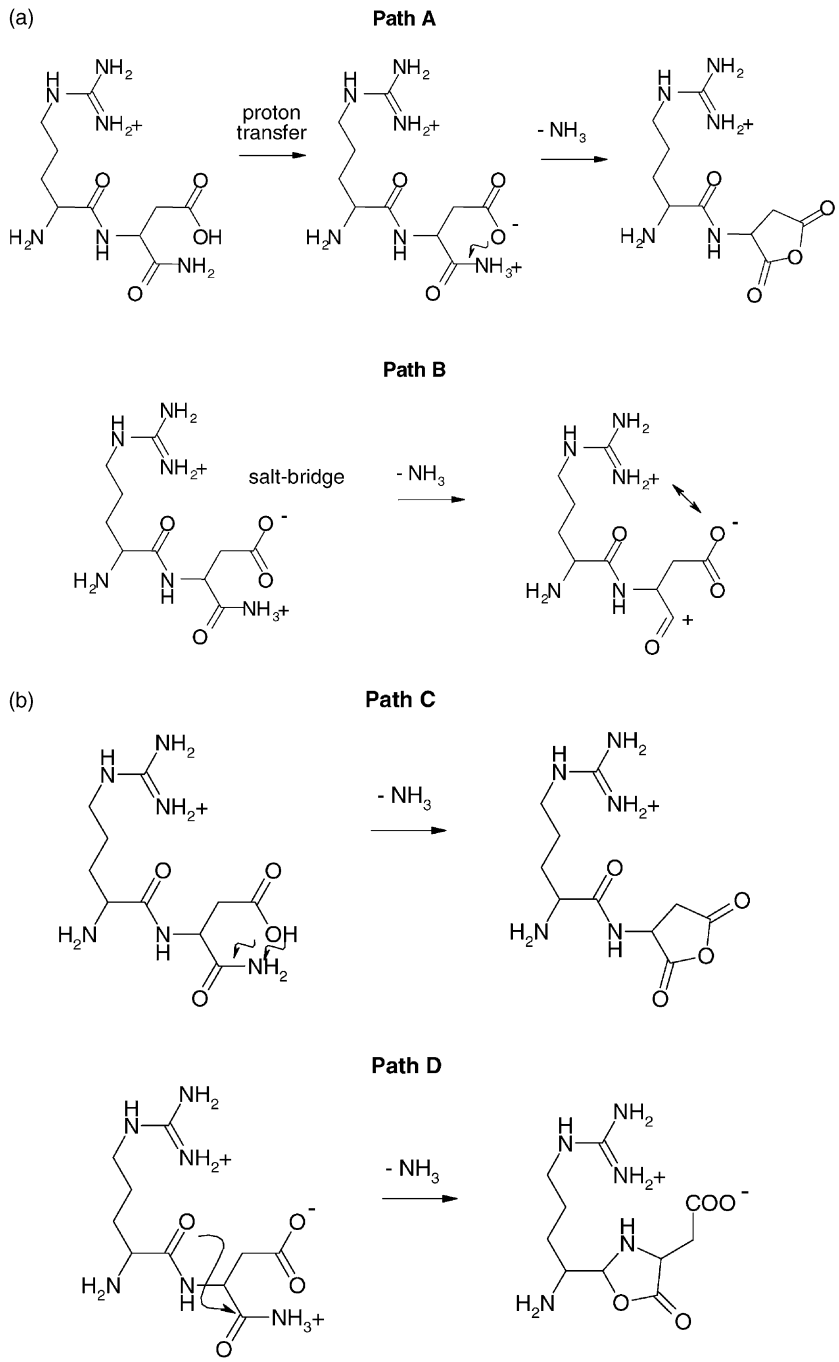
(a)
Path A
proton transfer
- NH3
Path B
salt-bridge
- NH3
(b)
Path C
- NH3
Path D
- NH3

Scheme 1.

Price et al. [4] have investigated the dissociation of the +11 ion of ubiquitin using blackbody infrared radiative dissociation (BIRD). These authors have found that ubiquitin^{11+} fragments nearly exclusively produce the y_{24}^{4+}/b_{52}^{7+} complementary ion pair. This fragmentation has been attributed to the Asp(52) residue of ubiquitin and explained by a mechanism (Scheme 1a, Path B, compiled for RD-NH_2) slightly different from that proposed by Yu et al. [1]. The first step of this mechanism is again a proton transfer from the aspartic acid side-chain to the neighboring amide nitrogen. The only difference between the first steps of Path A and B (Scheme 1a) is that Price et al. [4] assume that a protonated arginine side-chain nearby stabilizes the COO^- group of the aspartic acid side-chain by forming altogether a (+)(−)(+) salt-bridge, while Yu et al. [1] do not consider such an effect contrary to the fact that their peptides also contain protonated R or K side-chains. In the second step of Path B direct bond cleavage of the amide bond adjacent to the aspartic acid residue occurs. Price et al. [4] have also obtained useful kinetic information on this process using the BIRD technique. They have found that the rate limiting step of a possible complex reaction scheme has a very high frequency factor indicating an entropically highly favored mechanism such as a direct bond cleavage of the amide bond adjacent to the aspartic acid residue. Also, these authors assume that a relatively long living intermediate—that is formed by the interaction of the side-chain of Asp(52) and the protonated nitrogen of the adjacent amide bond—is formed in a faster reaction than the dissociation of the amide bond. (As far as terminology is concerned, we note here that we use the term "zwitterion" to describe the local interaction between the protonated arginine side-chain and the deprotonated carboxyl group of the aspartic acid side-chain. On the other hand, protonated species, in which such a local zwitterionic interaction exists, are hereafter called salt-bridged (SB) structures (i.e., the term "SB structures" is used for "protonated zwitterions"). Although these structures may not necessarily be "linear" SB structures and, as will be shown below, in most of the SB species, the mobile proton does not take part in the stabilization of the zwitterionic moiety, overall they have the characteristic (+)(−)(+) arrangement. The use of the "zwitterionic" term for these structures may be misleading because all these species are protonated structures and not neutrals.)

Selective cleavages at acidic residues (D, E, and C^*) in R containing and fixed charged derivatized peptides have been systematically studied recently by the groups of Wysocki and collaborators (see, [5–7] and references therein). These authors have investigated the fragmentation behavior of protonated peptides containing both basic and acidic amino acids under different experimental conditions and provided general rules to explain their observations. They concluded that non-selective cleavages along the peptide backbone occur when the number of ionizing protons exceeds the number of arginine residues, while dominant (selective) cleavages adjacent to the acidic residues predominate when the number of ionizing protons equals the number of arginine residues [5].

In the present study, we chose RD-NH_2 as a first model system to investigate the structural details of the mechanism of selective cleavages in protonated peptides containing both basic and acidic amino acid residues. RD-NH_2 is one of the simplest RD containing peptides, which is suitable to study by both MS/MS and high level of ab initio calculations. The main goals of the present study are as follows: (i) to obtain absolute and relative energies of all the important structures for $[RD\text{-}NH_2 + H]^+$, (ii) to specifically study SB and internally solvated (IS) structures and their possible conversions (if any), and (iii) to suggest pathways for the loss of NH_3 from the amide terminus of the peptide. We should note here that this way we try to model the specific cleavage of amide bonds adjacent to the aspartic (D) acid residues (towards the C terminus). Therefore, in the present paper, our goal was not to explain the MS/MS spectra by theoretical calculations, and, especially, not to investigate the loss of ammonia from the side-chain of arginine, even though this could be an important process in R containing peptides. (Although the loss of NH_3 from the Arg side-chain of protonated RD-NH_2 is an important process, we have evidence that loss of NH_3 also occurs from the

amide terminus (see below).) The loss of NH_3 from the arginine side-chain is the subject of a related study we are currently working on [21] using a model system RG-OH. Other related investigations are also underway in our laboratories on other model peptides, such as RC^*NH_2, RGD-NH_2, RGC^*NH_2, and RDGDR-OH.

2. Computational details

To scan the potential energy surface (PES) of protonated RD-NH_2 we applied our recently developed [22] conformational search engine devised specifically to deal with protonated peptides. These calculations start with molecular dynamics simulations on the target systems using the InsightII program (Biosym Technologies, San Diego, USA) in conjunction with the CVFF or AMBER force fields as implemented. Following an initial equilibration of 500 fs at 800 K, a 40 ps simulation is carried out at the same temperature. During the dynamics we saved structures in every 50 fs for further refinement by full geometry optimization using the same force fields. This way, 800 optimized structures are collected. In the next step of the scan these structures are analyzed by using our own conformer family search program. This program is able to group optimized structures into families for which the most important characteristic torsion angles of the molecule do not differ too much from each other (less than 2° from the minimum energy structure in each group). As an input of this program, the user has to specify the characteristic torsion angles to be monitored. After defining the conformer families, we usually appoint the most stable species in the families for further refinement at modest ab initio levels (HF/3-21G and HF/6-31G(d) in the present case). For all ab initio calculations the Gaussian 98 program [23] was used. Using scripts and small programs, input and running files are created which are executed on our HP or IBM-SP2 supercomputer systems. After completing the initial ab initio scans we build databases which contain the most important characteristics of the species determined, e.g., total and relative energies, selected geometry parameters, etc. The scan is finished by determining the equilibrium structure of the most stable species at higher levels of theory (B3LYP/6-31 + G(d,p) in the present case). In the final stage of the calculations we determine transition structures (TS) for the possible fragmentation channels. These calculations are usually carried out at high ab initio levels to obtain reasonable energetics of the process investigated.

Application of this strategy enables us to investigate the effect of protonation sites and isomerization states of protonated peptides in a very efficient way. Although the scheme outlined above is quite simple and very possibly finds most of the interesting conformers of the investigated species, its manual execution no doubt requires tremendous human effort. However, our implementation is optimized in the sense that nearly all the structure manipulations and transfers among program systems of different theoretical levels and also the generation and execution of the different files are highly automated.

The scan for the IS species of protonated RD-NH_2 was carried out exactly as described above. The dynamics simulation was initiated from a species protonated at the guanidine side-chain of the molecule. However, we had to face serious problems in the case of the SB structures. For these species, the guanidine and carboxylate side-chains of arginine and aspartic acid, respectively, are ionized and kept together as a local zwitterion. The extra proton can transfer to protonation sites of the backbone (such as N-terminal NH_2, amide O and N) so that, overall, a SB is formed (see comments on terminology in Section 1). Unfortunately, most of the available empirical force fields do not contain parameters for protonated amide nitrogen and oxygen. Furthermore, as was pointed out in our recent paper [14], it is not obvious how to consider all the important mesomer structures of nitrogen protonated amide bonds in the framework of force field methods. Because of these difficulties we decided to follow a slightly different strategy in the present case. First, we carried out molecular dynamics simulations for the neutral (net charge equal to zero) RD-NH_2 where the side-chains of arginine and aspartic acid were ionized and kept in a zwitterionic arrangement.

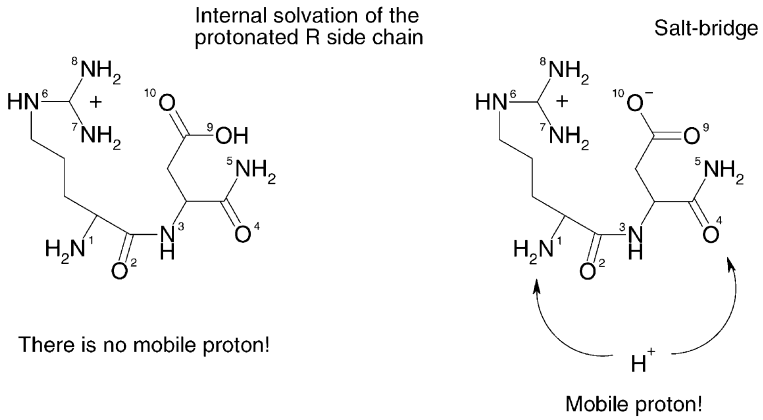

Scheme 2.

This simulation resulted in approximately 50 different zwitterionic structures. In the following steps, we protonated the possible backbone acceptor sites one by one (terminal NH_2, nitrogens and oxygens of the two amide bonds) of RD-NH_2 which resulted in approximately 400 initial structures. (The addition of proton to the terminal NH_2 and the nitrogens of the amide bonds is trivial. However, one can create a few reasonable candidates for each amide O protonated species. These candidates differ from each other only in the orientation of proton added.) All these structures were optimized at the HF/3-21G level of theory. Many of these optimizations led to already known and, in same cases, new IS structures. The latter is a clear indication of the fact that the initial scan of the PES by using molecular dynamics simulations is not perfect mainly due to the weakness of the applied MM parameter sets. Another part of the HF/3-21G optimizations resulted in interesting cyclic species which will be discussed later in detail. Only a fraction of the 400 species remained as a SB structure. The most stable species of each group were optimized again at the B3LYP/6-31 + G(d,p) level of theory.

Throughout the paper the following denotations are used. The first characters represent either IS of the proton or SB structures. In the case of the SB structures the position of the "extra" proton (i.e., that providing the net positive charge) is indicated by the next two characters. Because of the large number of different species obtained during the scan of the PES of protonated RD-NH_2, we had to drastically select amongst the structures for detailed discussion. (It is to be noted here that all species have been carefully investigated using visualization tools, etc.) The selection was made mainly considering the energy of the species obtained and higher energy structures are described in detail only if they are likely precursors for an isomerization or dissociation. Therefore, the order of total ab initio energies in the subgroup of species appointed for detailed description is indicated by letters in an alphabetical order. For example, IS_A represents the lowest energy structure of IS protonated RD-NH_2 and SB_N1_B represents the second lowest energy SB structure of the same compound carrying the extra proton on N1. The numbering of atoms is shown in Scheme 2 and also in Figs. 2–6.

3. Experimental details

3.1. Peptide synthesis

Protected Fmoc-amino acid derivatives were purchased from Advanced ChemTech (Louisville, KY), Chem Impex International (Wood Dale, IL), or American Peptide Company (Sunnyvale, CA). DMF was purchased from Fisher Scientific (Fair Lawn, NJ) and dried over 4 Å molecular sieves while nitrogen was

bubbled through it for at least 24 h prior use. All other starting materials were from Aldrich Chemical (Milwaukee, WI) unless otherwise noted, and used without purification. The protected linear sequences were assembled by solid-phase peptide synthesis, using the base-labile 9-fluorenylmethyloxycarbonyl (Fmoc) N^{α}-amino protecting group and acidolyzable *tert*-butyl and trityl type side-chain protecting groups. Manual solid-phase peptide syntheses were carried out in sterile plastic syringes containing porous polypropylene frits, starting with either Rink acid (Advanced ChemTech, 100 mg, 1.5 mmol/g loading) or Fmoc-Rink amide resin (American Peptide Company, 200 mg, 0.49 mmol/g loading). Fmoc deprotection was achieved by treatment with piperidine/DMF (1:4, 8 + 3 min), followed by washes with DMF (5 × 2 min). Fmoc-amino acids (Eq. (3) and (4)) were incorporated by 1-h couplings (completion verified by ninhydrin tests [24]) mediated by HBTU (Eq. (3))/HOBt (Eq. (3))/DIEA (Eq. (6)) in DMF. Prior to acid cleavages and deprotections the N-terminal Fmoc protecting group was removed manually by treatment with piperidine/DMF as reported above. Peptide chains were removed from the solid support with concomitant removal of all acid-labile side-chain protecting groups using TFA (Vega Biotechnologies, Tucson, AZ)/water/Et_3SiH (95:2.5:2.5, 1 mL) at 25 °C for 90 min. The filtrate was collected and combined with washes of neat TFA (2 × 2 mL) and concentrated by evaporation of the solvent under a constant stream of nitrogen. The crude cleaved peptides were precipitated by addition of cold Et_2O (∼15 mL) and centrifugation.

3.2. MS/MS measurements

Singly protonated RD-NH_2 was generated by ESI by direct infusion of ca. 50–80 μmolar solutions (in MeOH:H_2O 1:1 solvent) with a flow rate of 3 μL/min. The low-energy CID MS/MS (MS^2) spectra of $[M + H]^+$ ions, the MS/MS/MS (MS^3) spectra of $[MH\text{-}NH_3]^+$, and the MS^4 spectra of the $[MH\text{-}2NH_3]^+$ ions were obtained on a Thermoquest (Finnigan) LCQ instrument under standard operation conditions. The relative collision energies were slightly varied in the 10–25% relative energy range in order to detect the lowest energy fragmentation pathways.

4. Results and discussion

4.1. Structures of protonated RD-NH_2

The "IS" and "SB" structural variants of protonated RD-NH_2 are shown in Scheme 2. A very important difference between the IS and SB structures is that in the IS species, the proton is highly solvated but in the SB structures one ionizing proton is mobile and can "visit" different protonation sites. In the IS structures of protonated RD-NH_2 the protonated arginine side-chain can be solvated by the aspartic acid side-chain, the terminal NH_2 group and the oxygens of the amide bonds. The most important feature of the IS structures is that there is no mobile proton in this case that could initiate backbone dissociation to create structurally valuable fragment ions. Therefore, backbone fragment poor spectra is a clear indication of a population of protonated RD-NH_2 species where most of the ions are in the IS form.

However, due to the presence of both acidic and basic functional groups in the molecule, a strong interaction between the protonated arginine and deprotonated aspartic acid side-chains is also possible as shown in Scheme 2. In this case, the basic and acidic side-chains are kept together by very strong electrostatic and charge-transfer interactions (local "zwitterion"). Also, it is very possible that the existence of this local zwitterion has a large effect on the other (not very remote) parts of the molecule creating a pattern of very strong H-bonds. (As pointed out above, the SB structures can, therefore, be considered as "protonated" zwitterionic structures.) One of the most important features of the SB species is that a mobile proton is present in the ion, which can induce backbone dissociation. If the ion population contains a non-negligible amount of SB structures and the rigidity of the SB species does not prevent wandering of

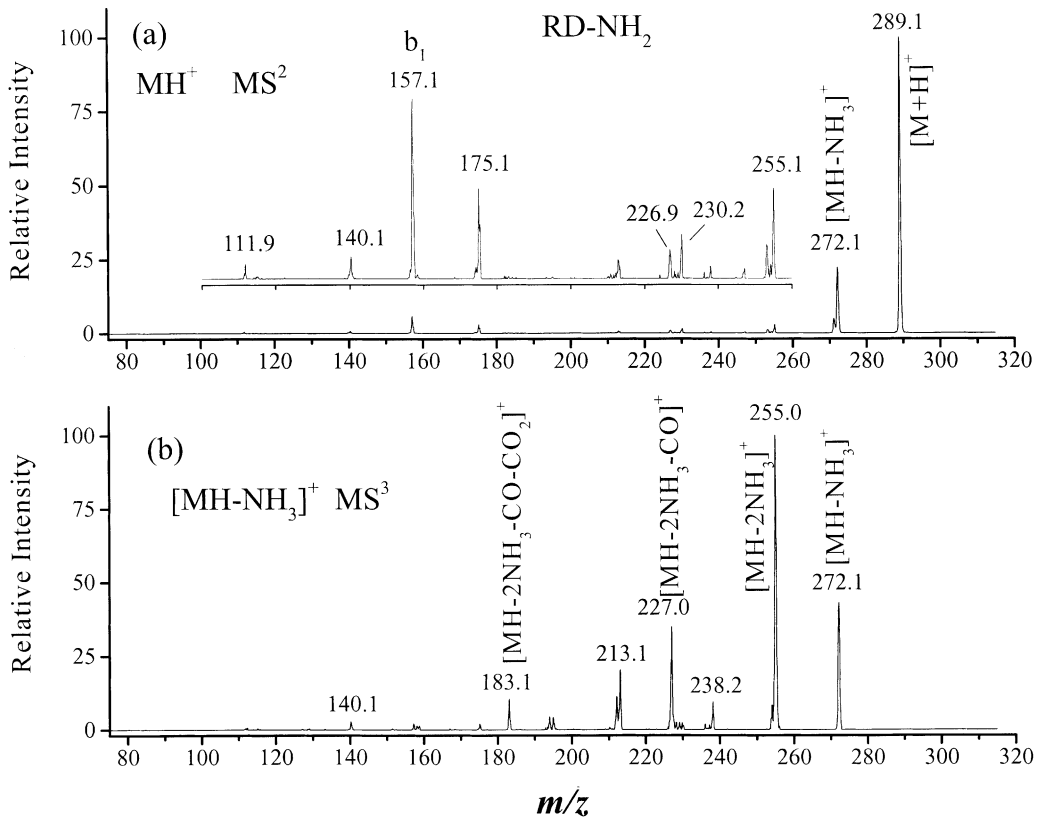

Fig. 1. Low-energy CID MS/MS spectra of (a) singly protonated RD-NH_2 $[MH]^+$ and (b) $[MH\text{-}NH_3]^+$. The MH^+ precursor ion was generated by ESI and the MS/MS (a) and MS/MS/MS (b) measurements were performed on a Finnigan LCQ instrument at 20 and 22% relative collision energies, respectively.

the extra proton amongst backbone protonation sites, the spectra of protonated RD-NH_2 will expectedly show the appearance of backbone fragment ions.

The low-energy CID MS/MS spectrum of singly protonated RD-NH_2 ($[MH]^+$ *m/z* 289) is shown in Fig. 1a, while Fig. 1b shows the MS/MS/MS (MS^3) spectrum of $[MH\text{-}NH_3]^+$ (*m/z* 272). At 20% relative energy in the Finnigan LCQ instrument, the main fragmentation process of $[MH]^+$ is the loss of NH_3 (Fig. 1a). Notice that the b_1 ion (*m/z* 157) is also observed with definitely smaller abundance than that corresponding to the NH_3 loss (*m/z* 272). The MS^3 spectrum of $b_1{}^+$ (not shown) shows extensive loss of NH_3 (*m/z* 140), loss of 42 (*m/z* 115), and loss of 45 (*m/z* 112). However, the fragment ion corresponding to the loss of 59 (*m/z* 98), which is characteristic for protonated guanidine of the R side-chain [25], is of very low intensity. We, therefore, suggest that most of the b_1 ions may not have an aziridinone structure but rather an eight-membered ring structure that is shown in Scheme 3. This ion can be formed from an amide nitrogen protonated species (Scheme 3) where the arginine side-chain is neutral, via nuclephilic attack of one of the nitrogens of the guanidine group on the carbon of the protonated amide bond. Note that such (usually high-energy) species are not described in the present paper but the formation of b_1 ions from protonated RG-OH is described in detail elsewhere [21]. Because of the special structure of the b_1 ion, the MS/MS spectrum of protonated RD-NH_2 does not directly indicate that SB species are present under the experimental conditions applied. (The eight-member ring b_1

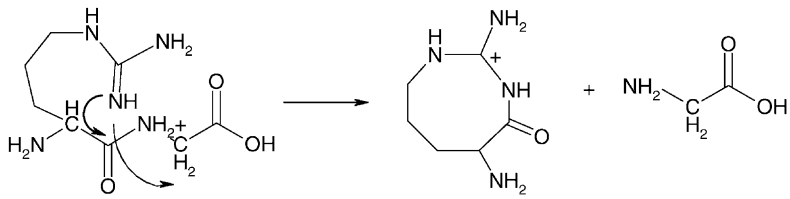

Scheme 3.

ions do not have to be assumed to originate from SB species.)

It is also worth noting that loss of ammonia from protonated RD-NH_2 is possible not only from the terminal amino group but also from the arginine side-chain. This latter reaction was investigated both experimentally and theoretically using model compounds like protonated R [25] and RG-OH [21]. These studies showed that the first step of NH_3-loss from the protonated guanidine group involves proton transfer reactions inside the guanidine moiety which result in a reactive configuration shown in Scheme 4. Loss of ammonia from this species occurs in a one-step process (Scheme 4) resulting in an ion having the carbodiimide moiety. The critical energy of NH_3 loss from the R side-chain of protonated RG-OH is 42.1 kcal/mol calculated at the B3LYP/6-31g(d) level of theory [21].

Based on the calculated critical energies presented below (and that of [21]) we suggest that ammonia losses from the arginine side-chain and from the terminal amide group have similar energetics and kinetics. Therefore, the population of $[MH\text{-}NH_3]^+$ ions of protonated RD-NH_2 may consist of at least two isomeric ions, one shown in Scheme 4 and the other originating from the cleavage of the terminal amide bond. This hypothesis can be proved considering that those $[MH\text{-}NH_3]^+$ ions which have the intact (protonated) guanidine moiety can fragment by loss of further NH_3 or neutral guanidine (59 loss). The MS^3 spectrum of $[MH\text{-}NH_3]^+$ ions shows a significant peak at *m/z* 213 (Fig. 1b). This peak can belong to the loss of 59 from the $[MH\text{-}NH_3]^+$ ions but it can also originate from the $[MH\text{-}2NH_3]^+$ ions at *m/z* 255, the fraction of which may have a 5-membered anhydride ring structure. However, in the MS^4 spectrum of $[MH\text{-}2NH_3]^+$ ions the fragment ion at *m/z* 213 is very weak. Therefore, we can conclude that the majority of ions at *m/z* 213 originate from the $[MH\text{-}NH_3]^+$ population by the loss of 59 which is characteristic for the protonated guanidine group. This observation suggests that at least a fraction of the $[M\text{-}NH_3]^+$ ions have an intact guanidine moiety, i.e., some of the NH_3 is lost by a bond cleavage at the amide N terminus.

The MS^3 spectrum obtained for $[MH\text{-}NH_3]^+$ contains several other fragment ions. The ions at *m/z* 255 (related to the loss of an additional NH_3), *m/z* 227 (formally a subsequent loss of CO from *m/z* 227), and *m/z* 183 (formally a subsequent loss of CO_2 from *m/z* 227) are worth mentioning at this point. Note that these subsequent losses have been proved by selecting and fragmenting $[MH\text{-}2NH_3]^+$ (spectrum not shown).

In the following we turn to the description of selected minima on the RD-NH_2 PES obtained from the scan described in Section 2 of the paper. Total and relative energies, structure determining factors, selected geometry parameters are listed in Tables 1 and 2. Note

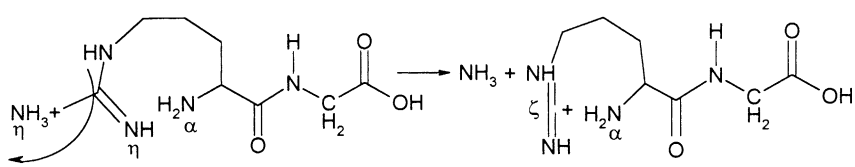

Scheme 4.

Table 1
Calculated total energies (E_{tot}, Hartree), relative energies (E_{rel}, kcal/mol), characteristic torsion angles (τ_x, degree) and selected interatomic distances (Å) of RD-NH_2 IS species

Species	E_{tot}	E_{rel}	τ_1	τ_2	τ_3	Selected interatomic distances (Å)
IS_A	−1023.089077	0.0	−24.4	−160.1	97.2	$r_{N3\cdots N1} = 2.680$, $r_{N6\cdots O10} = 2.884$, $r_{N7\cdots O10} = 2.826$, $r_{O9\cdots O4} = 2.581$, $r_{R-Damide} = 1.365$, $r_{Term.amide} = 1.342$
IS_B	−1023.088057	0.6	−21.8	71.4	166.9	$r_{N3\cdots N1} = 2.656$, $r_{N5\cdots O10} = 2.837$, $r_{N6\cdots O2} = 2.954$, $r_{N6\cdots O4} = 2.979$, $r_{N7\cdots O4} = 2.807$, $r_{R-Damide} = 1.354$, $r_{Term.amide} = 1.341$
IS_C	−1023.082659	4.0	15.7	−174.6	170.8	$r_{N6\cdots O2} = 2.750$, $r_{N7\cdots O10} = 2.894$, $r_{N3\cdots N1} = 2.650$, $r_{R-Damide} = 1.340$, $r_{Term.amide} = 1.357$
IS_D	−1023.081692	4.6	−166.9	−56.9	142.1	$r_{N3\cdots O10} = 2.782$, $r_{N6\cdots N1} = 2.870$, $r_{N7\cdots O2} = 2.905$, $r_{N7\cdots O4} = 3.232$ (pi–pi interaction), $r_{R-Damide} = 1.351$, $r_{Term.amide} = 1.355$
IS_E	−1023.07+9599	5.9	−168.5	−47.3	118.3	$r_{N6\cdots O9} = 3.002$, $r_{N7\cdots O10} = 2.873$, $r_{O4\cdots O9} = 2.450$, $r_{R-Damide} = 1.370$, $r_{Term.amide} = 1.337$
IS_F	−1023.076437	7.9	−28.3	−168.9	−171.0	$r_{N6\cdots O10} = 2.900$, $r_{N7\cdots O10} = 2.855$, $r_{N5\cdots O9} = 3.040$, $r_{N3\cdots N1} = 2.700$, $r_{R-Damide} = 1.360$, $r_{Term.amide} = 1.388$
IS_G	−1023.071324	11.1	19.4	−50.6	151.3	$r_{N7\cdots O4} = 2.869$, $r_{N6\cdots O2} = 2.764$, $r_{N3\cdots O10} = 2.839$, $r_{R-Damide} = 1.342$, $r_{Term.amide} = 1.353$
IS_H	−1023.065570	14.8	−17.4	−86.5	−168.1	$r_{N7\cdots O2} = 2.716$, $r_{N3\cdots O10} = 2.880$, $r_{R-Damide} = 1.341$, $r_{Term.amide} = 1.361$

For the numbering of the atoms, see Fig. 2a–h. The relative energies were calculated with respect to the total energy of the most stable species (IS_A) on the RD-NH_2 PES. Torsion angles τ_1, τ_2, and τ_3 correspond to the N1-$C^{\alpha R}$-C^{amide1}-N3, C^{amide1}-N3-$C^{\alpha D}$-C^{amide2}, and N3-$C^{\alpha D}$-C^{amide2}-N5 parameters, respectively.

Table 2
Calculated total energies (E_{tot}, Hartree), relative energies (E_{rel}, kcal/mol), characteristic torsion angles (τ_x, degree) and selected interatomic distances (Å) of RD-NH_2 salt-bridge and ring-containing species protonated at different positions of the peptide backbone

Species	E_{tot}	E_{rel}	τ_1	τ_2	τ_3	Selected interatomic distances (Å)	Position of H^+
SB_O2_A	−1023.069516	12.3	190.5	305.3	161.3	$r_{O2\cdots N1} = 2.528$, $r_{N6\cdots O9} = 2.751$, $r_{N7\cdots O10} = 2.787$	O2
SB_O2_B	−1023.068284	13.1	192.6	305.4	241.5	$r_{O2\cdots O4} = 2.473$, $r_{N3\cdots O9} = 2.650$, $r_{N5\cdots O10} = 2.952$, $r_{N6\cdots O9} = 2.760$, $r_{N7\cdots O10} = 2.838$	O2
SB_O2_C	−1023.059148	18.8	142.4	22.5	−179.1	$r_{O2\cdots O4} = 2.403$, $r_{N6\cdots O10} = 2.785$, $r_{N9\cdots O9} = 2.725$,	O2
SB_O4_A	−1023.067788	13.4	202.0	299.1	243.4	$r_{O4\cdots O2} = 2.463$, $r_{N6\cdots O9} = 2.775$, $r_{N7\cdots O10} = 2.870$	O4
SB_N1_A	−1023.064731	15.3	189.6	308.7	157.1	$r_{N1\cdots O2} = 2.452$, $r_{N3\cdots O9} = 2.576$, $r_{N6\cdots O9} = 2.721$, $r_{N7\cdots O10} = 2.739$	N1
SB_N1_B	−1023.056098	20.7	54.1	116.9	176.9	$r_{N1\cdots O9} = 2.540$, $r_{N1\cdots O4} = 2.884$, $r_{N6\cdots O2} = 2.875$, $r_{N7\cdots O10} = 2.686$	N1
SB_N3_A	−1023.037318	32.5	322.3	199.6	292.1	$r_{N3\cdots N1} = 2.741$, $r_{N3\cdots O9} = 2.550$, $r_{N5\cdots O9} = 2.964$, $r_{N6\cdots O10} = 2.816$, $r_{N7\cdots O9} = 2.887$	N3
SB_N5_A	−1023.037675	32.3	257.7	306.1	322.4	$r_{N5\cdots N1} = 3.049$, $r_{N5\cdots O9} = 2.562$, $r_{N6\cdots O9} = 2.879$, $r_{N7\cdots O10} = 2.751$	N5
Ring5	−1023.061960	17.0	21.7	73.4	152.4	$r_{N3\cdots N1} = 2.673$, $r_{N6\cdots O2} = 2.703$, $r_{N7\cdots O10} = 2.917$	O2 ring formation
Ring6	−1023.048145	25.7	54.3	71.2	143.1	$r_{N3\cdots N1} = 2.713$, $r_{O2\cdots O4} = 2.628$, $r_{N7\cdots O2} = 3.233$, $r_{N8\cdots O10} = 2.889$	O4 ring formation

For the numbering of the atoms, see Figs. 3a–g and 4a–b. The relative energies were calculated with respect to the total energy of the most stable species (IS_A) on the RD-NH_2 PES. Torsion angles τ_1, τ_2, and τ_3 correspond to the N1-$C^{\alpha R}$-C^{amide1}-N3, C^{amide1}-N3-$C^{\alpha D}$-C^{amide2}, and N3-$C^{\alpha D}$-C^{amide2}-N5 parameters, respectively.

that only a few characteristic low-energy structures are discussed here in detail. Although these structures represent only a small fraction of all the structures obtained during the (full) scan of the PES for protonated RD-NH_2, their selection based on their total energies is reasonable enough not to overlook significant structures that may be formed in the mass spectrometer.

4.1.1. IS ion structures of protonated RD-NH_2

Fig. 2a shows the lowest energy (B3LYP/6-31 + G(d,p)) structure of protonated RD-NH_2 (IS_A, for denotations here and throughout the paper, see Section 2). Note that the relative energies of all the other species discussed in this paper will be referenced to the energy of this species, IS_A. As expected, the added proton is located on the arginine side-chain. The protonated guanidine group is solvated by the carbonyl oxygen (O10) of the aspartic acid side-chain. The acidic proton of aspartic acid is in a strong H-bridge with the C-terminal amide oxygen (O4). The distance of the pillar atoms (O9 and O4) of the H-bond is extremely short (2.581 Å). For such strong H-bridges it is typical that the distortion of the proton from its equilibrium position is determined by a single-well potential. This implies that the bridged proton can be found close to O4 only with a small probability.

The second lowest energy structure (IS_B) is shown in Fig. 2b. The energy of this structure is higher by 0.6 kcal/mol than that of the lowest energy structure (Table 1). A significant difference between the structures IS_B and IS_A is that the acidic hydrogen of the aspartic acid is not involved in a H-bond in IS_B. Instead, the carbonyl oxygen of the aspartic acid side-chain (O10) is close enough to the nitrogen of the terminal amide bond (N5) to form a hydrogen bond. However, this interaction is quite weak compared to the COOH–guanidine interaction found in IS_A. This means that the side-chain of the aspartic acid residue can rotate more freely in IS_B than in IS_A. The protonated guanidine group is solvated by the two amide oxygens (O2 and O4) in IS_B. The involvement of the carbonyl oxygens in the solvation of the charge on the arginine side-chain has a characteristic effect on the amide bond lengths. For example, in IS_A there is no amide carbonyl interaction with the arginine side-chain, the R–D amide bond length is 1.365 Å while in IS_B the R–D amide bond length is 1.354 Å (Table 1). These results are in good agreement with those reported for variations in amide bond lengths *and* bond orders at a lower level of theory [9,10]. While the amide bond lengths and bond orders are evidently not the only factors which determine the mechanism and energetics of backbone fragmentation, it is clear that cleavage of a shorter amide bond with higher bond order can be assumed to require larger activation energies.

It is worth noting here that we found a large number of species similar to IS_A and IS_B in the internal energy range of 0–10 kcal/mol. These structures are not discussed in detail to save room for the description of the more important mechanistic aspects of fragmentation of protonated RD-NH_2.

In Fig. 2c we show a species (IS_C) where the protonated guanidine group is solvated by the oxygen of the R–D amide group (O2) and the carbonyl oxygen of the aspartic acid side-chain (O10). The relative energy of IS_C is low at 4.0 kcal/mol compared to that of IS_A. Note again that there is substantial difference between the lengths of the amide bonds (Table 1). The R–D peptide bond (1.340 Å) which is involved in the solvation of the protonated guanidine moiety is shorter than the terminal one (1.357 Å). This species is a likely candidate for an IS $\Leftrightarrow$ SB transition which will be discussed in more detail below.

In the structure of IS_D (Fig. 2d) the N-terminal NH_2 group (N1) is also involved in the solvation of the protonated guanidine moiety. The relative energy of IS_D is 4.6 kcal/mol showing that solvation of the protonated guanidio group is less favored by the NH_2 group than by the carbonyl oxygens. It is also interesting that the arginine side-chain is solvated not only by H-bonds but also via charge-transfer interaction between the terminal amide oxygen (O4) and the protonated guanidine group (Fig. 2d). On the other hand, the aspartic acid side-chain is involved in a quite weak N(3)–H$\cdots$O(10) hydrogen bond allowing nearly free rotation around the C^{α}–C^{β} bond.

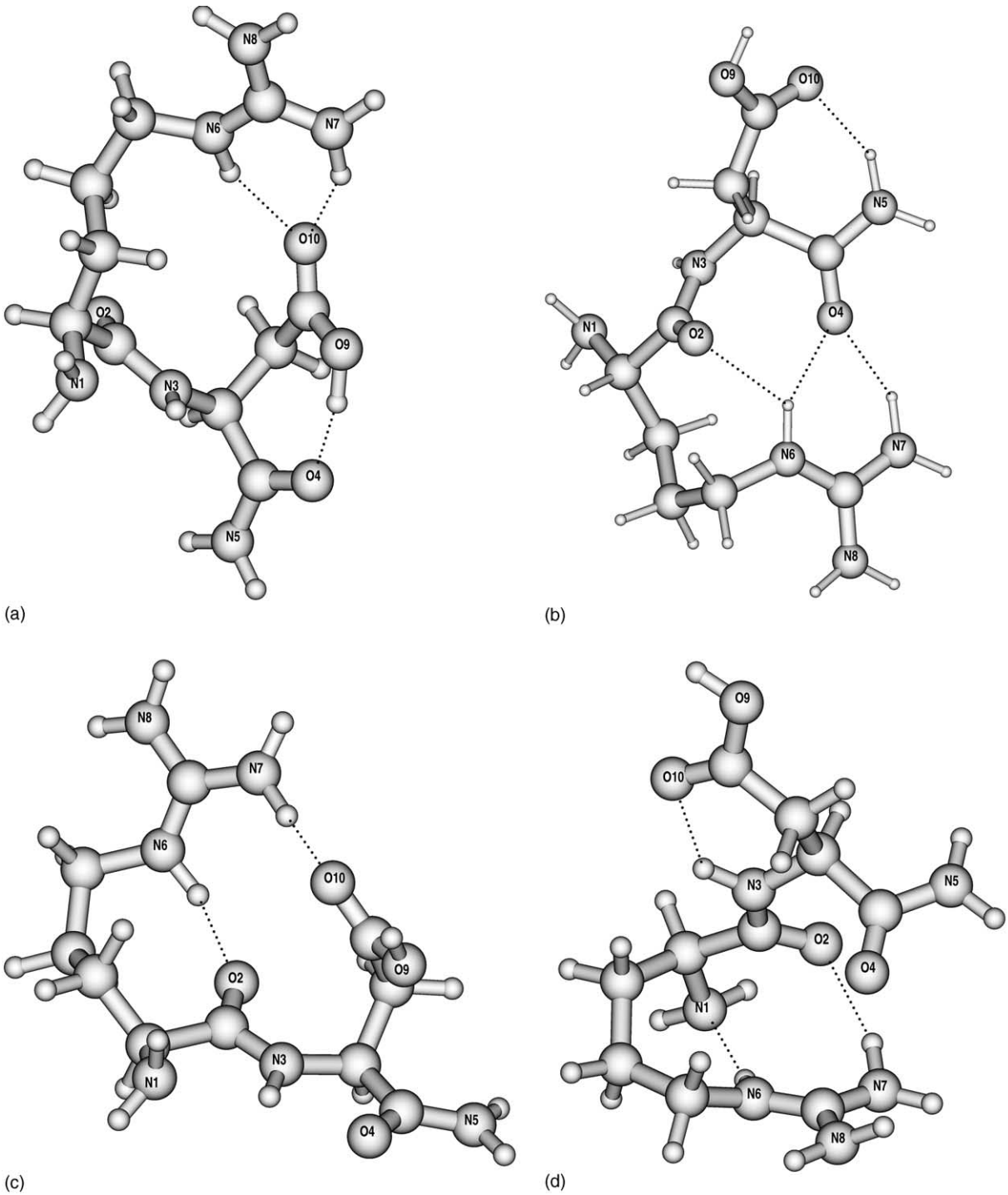

Fig. 2. Selected characteristic IS structures. The lowest energy species is IS_A ($E_{rel} = 0.0$ kcal/mol) and the relative energies of the species are increasing in alphabetical order. (For the detailed description of denotations, see Section 2.)

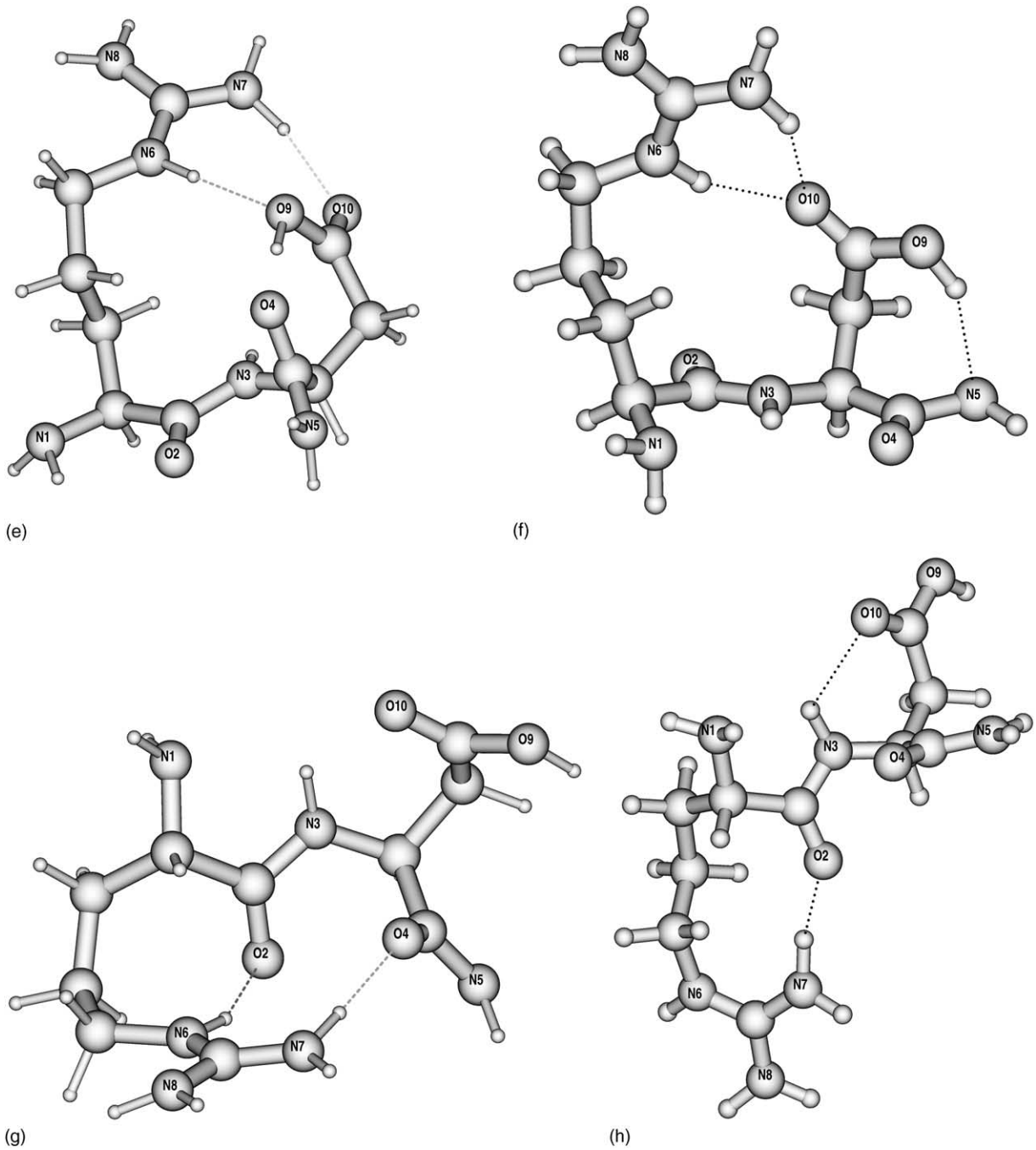

Fig. 2. (*Continued*).

From the structure IS_E shown in Fig. 2e (5.9 kcal/mol relative energy, Table 1) a SB structure can also be generated by transferring the acidic hydrogen of the aspartic acid side-chain (O9–H) to the carbonyl oxygen of the R–D amide bond (O4). (For more detailed discussion of the mechanism and energetics of this proton transfer, see below.)

In species IS_F shown in Fig. 2f the protonated guanidine group is solvated by the side-chain of the aspartic acid residue (O10). IS_F is quite similar to IS_A, the main difference between the two species is that the acidic hydrogen points toward the nitrogen of the terminal amide bond (N5) in IS_F instead of the amide oxygen of IS_A (O4). Of course, the amide nitrogen is less efficient H-bond acceptor than the amide oxygen resulting in a 7.9 kcal/mol relative energy of IS_F (Table 1). On the other hand, the O(9)–H$\cdots$N(5) hydrogen bond generates a rather long terminal amide bond (1.388 Å). Loss of ammonia from IS_F will be discussed below.

In the structure of IS_G depicted in Fig. 2g, the protonated guanidino group is solvated by the two amide oxygens (O2 and O4, 11.1 kcal/mol relative energy, Table 1). The carbonyl oxygen of the aspartic acid side-chain (O10) is close to the hydrogen of the R–D amide bond (N3–H). Due to this interaction, the hydroxyl OH of the COOH moiety (O9) is located quite close to the carbon of the terminal amide bond, and the OH bond is nearly parallel to the terminal amide bond. This structure is a likely precursor of a four-center-one-step (FCOS) reaction that would lead to loss of ammonia from the amide terminus. The details of this dissociation will be discussed below.

Similar to IS_G, species IS_H shown in Fig. 2h is also a likely precursor for a FCOS reaction leading to loss of ammonia (14.8 kcal/mol relative energy, Table 1). The most important difference between IS_G and IS_H is that in IS_H the protonated guanidine group is solvated only by the R–D amide oxygen (O2) and the terminal amide bond is longer in IS_H (1.361 Å) than what is calculated in IS_G (1.353 Å). On the other hand, in IS_H, the carbonyl oxygen of the aspartic acid side-chain (O10) is H-bonded to N3–H of the R–D amide bond. Details of the corresponding reaction will be discussed below.

Note that a large number of structures have been found in which the acidic proton of the COOH group is directed to possible protonation sites of the backbone. Examples are shown in Fig. 2a, e, and f. In most of these cases, the pillar atoms of the H-bridge are quite close to each other. This means that the (acidic) hydrogen involved moves according to a single-well potential. In such a situation, the hydrogen stays in the close proximity of the backbone protonation site with a small but finite probability. If it does so, an IS $\Leftrightarrow$ SB transition is possible by an appropriate internal rotation. A few examples of this type of processes will be discussed below.

4.1.2. SB structures of protonated RD-NH_2

As described above, SB formation is possible for protonated RD-NH_2 via a transfer of the acidic proton of the aspartic acid side-chain to the backbone. (In this case, the ionizing proton is formally assumed to be located on the R side-chain.) In the following we describe the most important energetic and structural features of various SB structures obtained from the scan of the PES of protonated RD-NH_2 (for energetic and geometric data, see Table 2).

Fig. 3a shows the most stable SB structure (SB_O2_A) where the "acidic" proton is located on the oxygen of the R–D amide bond (O2). The protonated carbonyl oxygen is stabilized by a strong H-bond formed by the terminal amino group (N1). The relative energy of SB_O2_A is only 12.3 kcal/mol (Table 2) with reference to IS_A (Table 1). This is due to the strong H-bonds stabilizing both the "local" zwitterion and the protonated carbonyl oxygen. Protonated RD-NH_2 ions have no doubt larger internal energy than 12.3 kcal/mol under the usual ion activation (tandem MS) conditions giving rise the possibility of SB formation in the gas-phase. A similarly low-energy structure (SB_O2_B, 13.1 kcal/mol relative energy, Table 2) was found in which the carbonyl oxygen of the terminal amide bond functions as a H-bond acceptor stabilizing the protonated amide oxygen (figure not shown). It is worth noting here

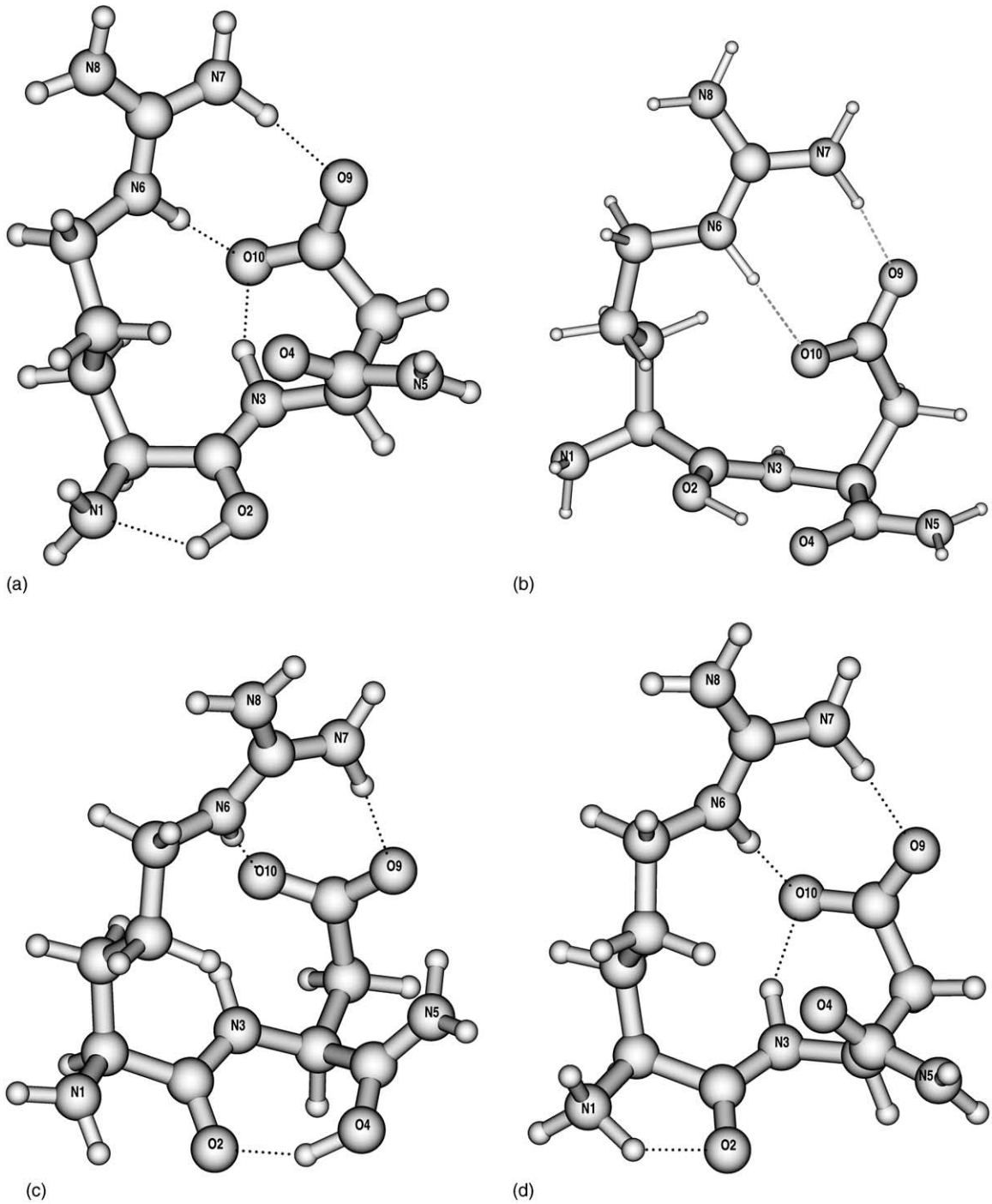

Fig. 3. Selected characteristic SB structures. The atomic symbol and number indicates the protonation site in these structures. (For the detailed description of denotations, see Section 2.)

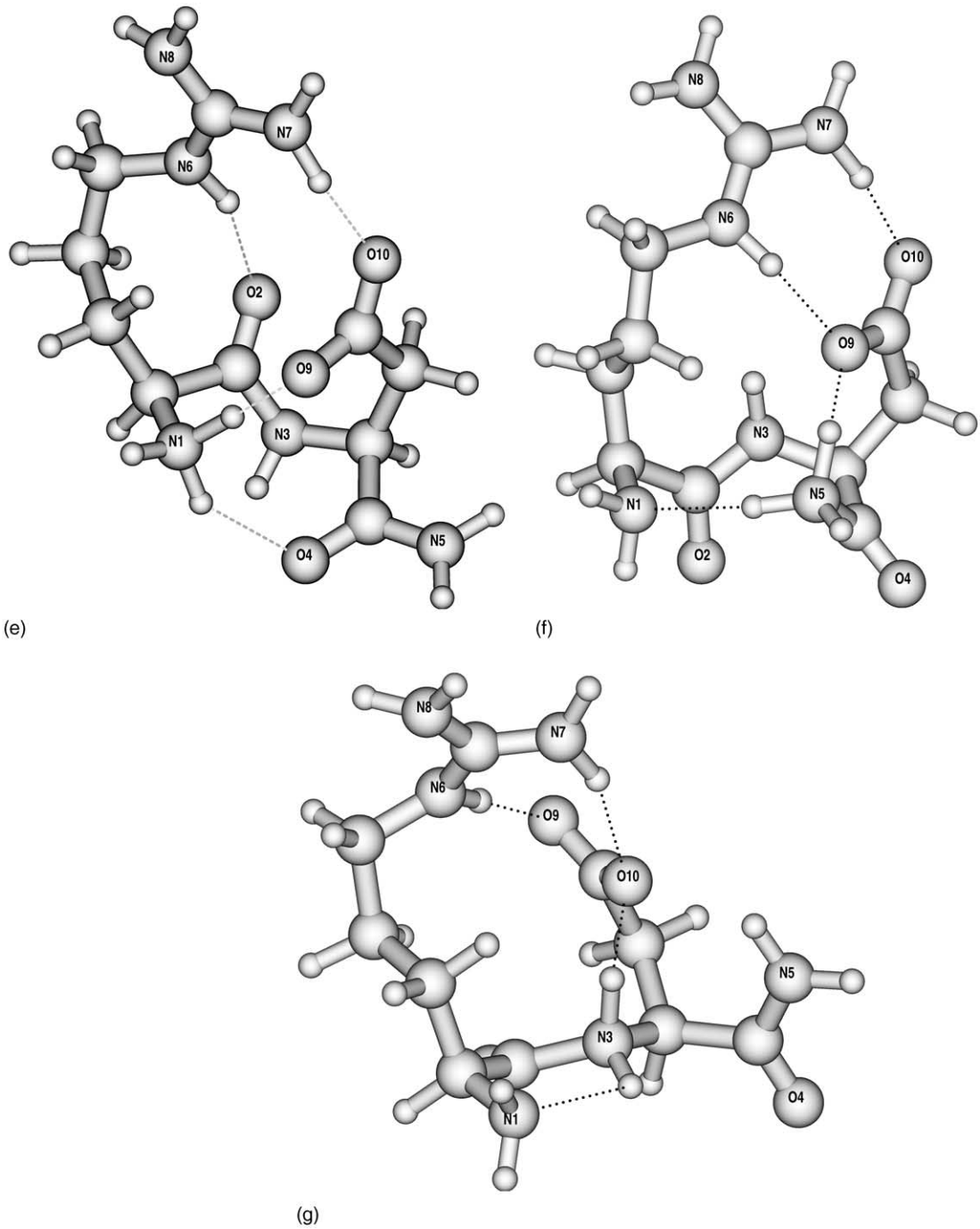

Fig. 3. (*Continued*).

that a small barrier was found [14] for proton transfer (PT) reactions between two adjacent amide oxygens in the case of protonated formyl-glycine-amide indicating very fast proton transfer. Also, we found a fast proton transfer between the terminal NH_2 and the amide oxygen of protonated diglycine (GG) for an arrangement of the backbone atoms similar to that of SB_O2_A [15]. It is also interesting that there is no direct interaction between the zwitterion moiety of the molecule and the protonated carbonyl oxygen in either cases. The carboxylate group of the acidic side-chain is further stabilized by interacting with the R–D amide N(3)H group (Fig. 3a).

Fig. 3b shows SB_O2_C lying at 18.8 kcal/mol relative energy (Table 2). The structure of SB_O2_C is very similar to that of SB_O2_B. We present SB_O2_C because there is a one-step reaction between this species and IS_E (Fig. 2e) due to the fact that the mobile proton on the backbone of RD-NH_2 is quite close to the zwitterion itself in SB_O2_C. This transition will be discussed in detail in Section 4.2.

Similar to the O2 protonated SB species, the SB_O4 structures have low relative energies due to the complex internal H-bond system formed, as demonstrated in SB_O4_A (Fig. 3c, 13.4 kcal/mol relative energy, Table 2). In this case, the protonated carbonyl oxygen (O4) is stabilized by the R–D amide oxygen (O2). As we showed for the case of protonated formyl-glycine-amide [14], proton transfer is very fast between the two adjacent amide oxygens (SB_O2_X $\Leftrightarrow$ SB_O4_Y transitions) in a structurally similar arrangements of the corresponding atoms. Again, there is no "direct interaction" between the zwitterion and the extra proton at the backbone protonation site (O4).

Fig. 3d shows another SB structure (SB_N1_A) where the extra proton is located at the N-terminal NH_2 group (N1). This protonation site is stabilized by a strong H-bond including the O2 R–D amide oxygen. Proton transfer to the O2 atom requires (to reach species, SB_O2_A) only a few kcal/mol extra energy for protonated GG for the same arrangement of the corresponding atoms [15]. The carboxylate group involved in the zwitterion is in a H-bond with the R–D amide NH group (N3). The relative energy of SB_N1_A is only 15.3 kcal/mol (Table 2).

Fig. 3e shows a structure (SB_N1_B) lying at 20.7 kcal/mol relative energy (Table 2) that is quite similar to IS_C (Fig. 2c). Actually, there is a one-step transition (a proton transfer) between SB_N1_B and IS_C. This reaction will be discussed in details in Section 4.2.

Fig. 3f shows a very important structure (SB_N5_A) at 32.3 kcal/mol relative energy (Table 2). Here, protonation occurs on the nitrogen of the terminal amide bond (N5) and the resulting NH_3 group is involved in a strong H-bond with the carboxylate (O9) of the SB. The protonated amide nitrogen (N5) is also involved in another strong H-bond formed with the N-terminal NH_2 group (N1). Actually, this is the structure which appears as the second species, the intermediate, of the mechanism proposed by Yu et al. [1] and Price et al. [4] (Scheme 1a, Paths A and B). A more detailed discussion of possible fragmentation pathways including SB_N5_A will be given below.

Fig. 3g shows a SB species (SB_N3_A) lying at 32.5 kcal/mol relative energy (Table 2) in which the extra proton is carried by the nitrogen of the R–D amide bond (N3). The protonated amide nitrogen is stabilized by strong H-bonds with both the caboxylate group of the aspartic acid side-chain (O10) and the N-terminal NH_2 group (N1).

Summarizing our results obtained for the SB species one can draw the following conclusions. All the SB structures are stabilized by strong H-bonds and, in some cases, intramolecular charge-transfer interactions. The number of intramolecular H-bonds for an average SB species is definitely larger than what we found for the IS RD-NH_2 structures. This results in "highly packed" SB structures with possibly substantial entropy effects. This entropy effect increases with the size of the molecule making the formation of SB structures less favorable for larger analogs of RD-NH_2.

A summary of the energetics of SB structures with the extra proton locating at different backbone protonation sites is shown in Scheme 5. The relative energies of the most stable species of a given subgroup

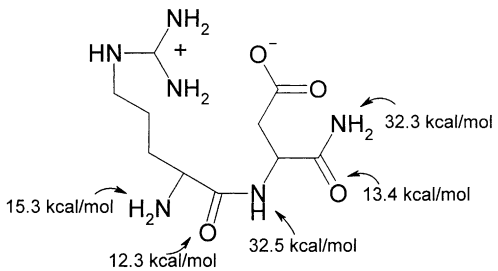

Scheme 5.

(for example SB_O2_A) is noted at the particular protonation site. (As mentioned above, the relative energies are referenced to the energy of the most stable species, IS_A.) The most stable SB structure belongs to protonation at the oxygen of the R–D amide bond (O2). Protonations of the N-terminal NH_2 group (N1) and the oxygen of the C-terminal amide (O4) require approximately the same internal energy. On the other hand, proton transfers to the amide nitrogens require substantially larger internal energy of about 32 kcal/mol. Although these are energetically quite high lying species, their formation is possible under usual ion activation (tandem MS) conditions in mass spectrometers. Proton transfer reactions connecting various SB species are probably fast. Note, however, that H/D exchange experiments performed in our laboratory for protonated RD-NH_2 did not result in any H-D exchange. This is in agreement with the calculations, i.e., the SB structures are not formed in a *great extent* during the electropray ionization. (As mentioned above, the formation of SB structure are, nevertheless, still possible under ion activation.)

The number of SB structures we found during the scan of the PES of protonated RD-NH_2 is much smaller than the number of corresponding IS structures. This may be due to the fact that the carboxyl group of the aspartic acid side-chain is not a strong acid. Therefore, optimizations of most of the initial structures where protonation occurred on the backbone of the *neutral* SB species led to IS structures. (The acidic proton transferred back to the carboxylate group of the D side-chain.) Furthermore, the optimization of these structures led also, in some cases, to interesting cyclic structures which will be discussed in the following.

4.1.3. *Cyclic structures of protonated RD-NH_2*

The cyclic structures (Ring5 and Ring6, respectively) obtained from the PES scan described above are shown in Fig. 4a and b. (Only two examples are given to save space for discussions on the mechanistic aspects of the fragmentation of protonated RD-NH_2.) Total and relative energies, structural information including selected geometry parameters are also collected in Table 2 for these species. We obtained the geometries shown in Fig. 4a and b from optimizations initiated from SB species where the extra proton was located on the terminal amide oxygen (O4) and the oxygen of the R–D amide bond (O2), respectively. The presence of a protonated amide oxygen makes the carbon of the amide bond even more positive than its neutral counterpart. Such a carbon is an excellent target of any nucleophilic attack. On the other hand, the negatively charged carboxylate of the SB can be considered as a nucleophilic intramolecular reaction partner. Therefore, in many of the cases when the location of the protonated amide bond and the carboxylate makes it possible, a five- or six-member ring was formed during the geometry optimizations. These cyclic structures do not contain a SB any longer. Rather, the protonated guanidine moiety is stabilized by strong H-bonds including the oxygens of the newly formed ring and the backbone of the molecule (O10 and O2, respectively). The relative energy of the most stable cyclic isomer (Ring5) is 17.0 kcal/mol with reference to IS_A (Table 2), which is larger than that of the most stable SB species (SB_O2_A, 12.3 kcal/mol, Table 2). Also, formation of the five- or six-membered rings needs large internal energies (i.e., the calculated barriers to the ring formation are larger than the barriers required for the IS $\Leftrightarrow$ SB transitions), so we do not discuss these species in detail. Only note, for example, that a one-step transition occurs between species IS_A (Fig. 2a) and Ring5 (Fig. 4a). The relative energy of the corresponding TS (IS_A_Ring5, Fig. 4c) is 29.6 kcal/mol which is definitely higher than those TSs that connect the IS and SB species (see below).

Nevertheless, the formation of the cyclic species should be considered as a competitive process of the IS ⇔ SB transitions and the fragmentation channels. On the other hand, one can also consider the cyclic species as intermediers of the IS ⇔ SB transitions since it is possible that the proton located, e.g., on O4 in Ring5 transfers to other backbone protonation sites with simultaneous opening of the five-membered ring.

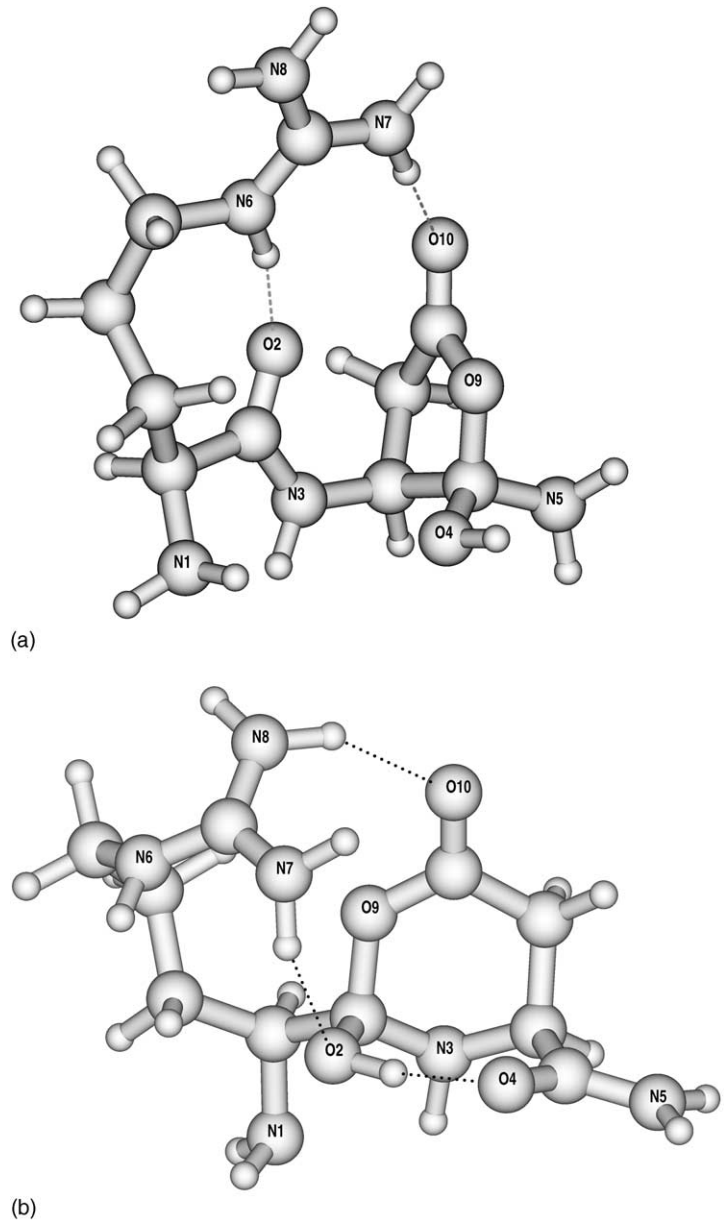

Fig. 4. A five (a) and a six (b) member ring cyclic structure of protonated RD-NH_2, and a corresponding "IS_A_Ring5" transition state (c). (For the detailed description of denotations, see Section 2 and text.)

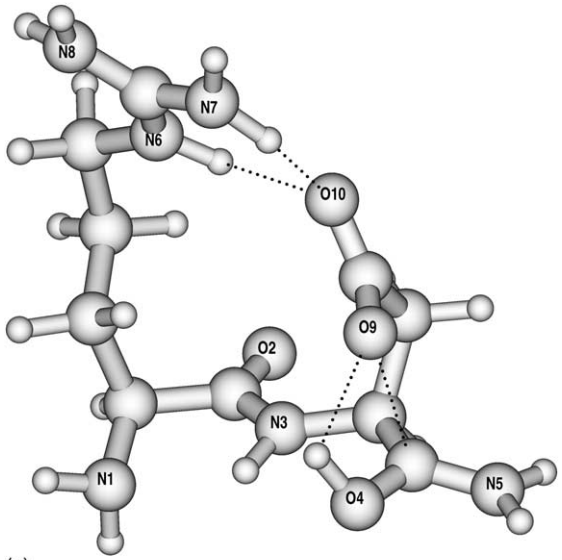

Fig. 4. (*Continued*).

We believe, that while such processes cannot be excluded based on the available computational data, the cyclic species on the PES of protonated RD-NH_2 do not play a significant role in the fragmentation of the parent ion. Therefore, instead of a detailed description of the formation and the fate of the cyclic species, we turn to the discussion of the more important competitive processes, the IS ⇔ SB transitions themselves.

4.2. Transitions between the IS and SB species

Having described the structures and relative energies of several IS and SB species, we investigate the factors that determine the mobilization of the acidic proton of the aspartic acid side-chain, i.e., possible transitions between the IS and SB structures. In the calculations for the IS ⇔ SB isomerization, we assumed that the transfer of the acidic proton to one of the protonation sites of the backbone of RD-NH_2 and the formation of a zwitterionic structure between the protonated guanidine and the carboxylate groups take place in a concerted manner. Therefore, we selected those IS structures for detailed investigation where the COOH moiety of the aspartic acid residue solvates the protonated guanidine group. It is worth noting here that the strong interaction between the protonated guanidine group and COOH weakens the carboxylate O-H bond making the transfer of the COOH proton more feasible. Another structural criteria for a successful IS ⇔ SB transition is that the acidic H of the COOH group must be involved in a H-bridge with one of the possible protonation sites of the backbone of RD-NH_2. As mentioned above such hydrogen bonds are usually quite strong and the hydrogen involved experiences a single-well potential. In such circumstances, the acidic proton can be found only with a small probability close to the backbone protonation site. However, if the proton stays close to the backbone site and an appropriate internal rotation takes place simultaneously, an IS ⇔ SB transition can occur. Of course, it is important to stabilize *both* the zwitterion just formed and the protonated backbone site to make the IS ⇔ SB transition energetically favorable. A good example for the lack of stabilization is the global minimum structure (IS_A, Fig. 2a) on the PES of protonated RD-NH_2. At first sight, it seems to be a promising candidate for a IS ⇔ SB transition because the protonated guanidine group is solvated by the COOH group and the acidic hydrogen is involved in a H-bridge with the O9 and O4 pillar atoms. However, after the transfer of the acidic proton to O4, there is no electron-rich group in the proximity of O4 that could stabilize the protonated terminal amide oxygen (O4). (A possible stabilization by the nearby NH_2 (N5) group is not strong enough.)

Species IS_E shown in Fig. 2e satisfies all the above conditions. The protonated guanidine group is stabilized by the side-chain of the aspartic acid residue and the acidic H is involved in a strong H-bridge with the O4 and O9 pillar atoms. Also, the oxygen of the R–D-amide bond (O2) is relatively close to the O4 group providing stabilization for the proton while it is located close to O4. The calculated transition structure (IS_SB_1) for this IS ⇔ SB transition is shown in Fig. 5a. The acidic proton transferred to the oxygen of the terminal amide bond (O4) is stabilized by the oxygen of the R–D amide bond (O2). The relative energy of IS_SB_1 is relatively high at 27.4 kcal/mol

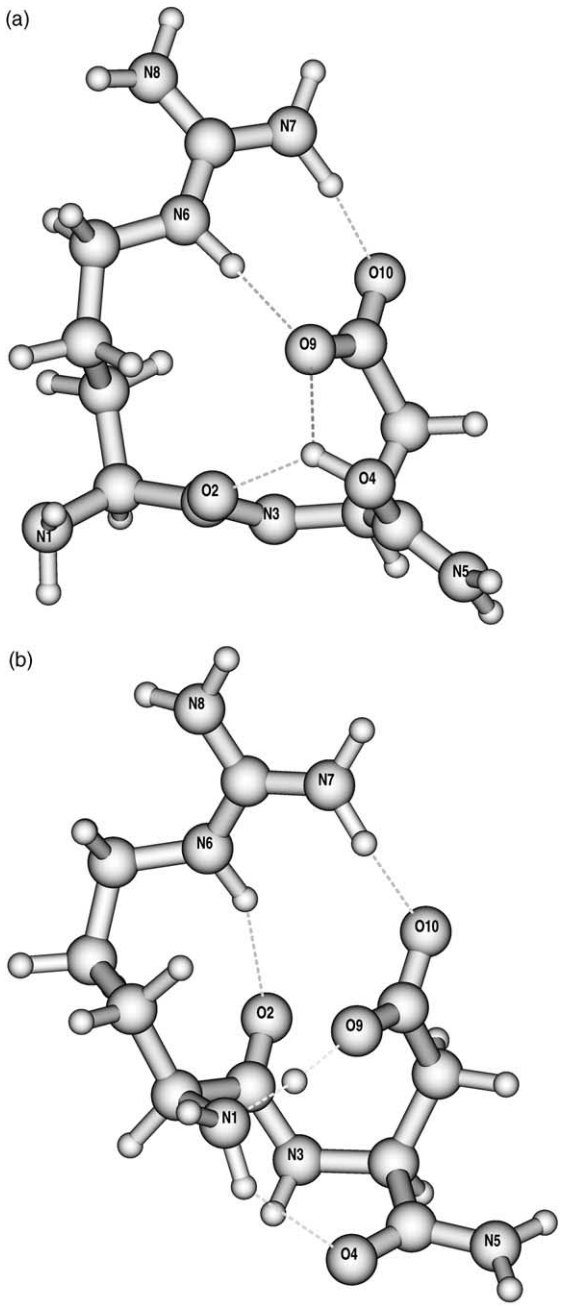

Fig. 5. Two possible transition state structures for the IS ⇔ SB transition. (a) The acidic proton is transferred to the oxygen of the terminal amide bond (O4), IS_SB_1 transition, and (b) the proton from the terminal amino group (N1) is transferred to the carboxylate group of the Asp side-chain, IS_SB_2 transition. (See text, for details.)

(Table 3) suggesting that the acidic proton of COOH is much less mobile than the proton added to peptides containing no arginine residue. On the product side of the minimum energy path we found SB_O2_C shown in Fig. 3b. It is interesting that the acidic proton transfers further from O4 of TS IS_SB_1 to the oxygen of the R–D amide bond (O2). The relative energy of species SB_O2_C is 18.8 kcal/mol slightly higher than that of the most stable SB_O2 species, SB_O2_A (12.3 kcal/mol, Table 2). However, their structures are quite similar and only a few, very likely low-energy, internal rotations are needed for their interconversion.

We also tried to find possible IS ⇔ SB transitions starting searches from various SB species. Of course, not all of the SB species are likely candidates for such transitions. The most important requirement in this respect is that the mobile proton on the backbone of RD-NH_2 should be close to the SB. As mentioned above, this is usually not the case. In most of the SB species, the mobile proton does not take part in the stabilization of the zwitterionic moiety. One of the exceptions (SB_N1_B) lying at low relative energy (20.7 kcal/mol, Table 2) is shown in Fig. 3e where the protonated guanidine group is solvated by the oxygen of the R–D amide bond (O2) and one of the oxygens of the COO^- group (O10). The protonated amino terminus is H-bonded to both O9 of the COO^- group and the terminal oxygen (O4). In such circumstances, one of the protons of the terminal amino group can transfer to the carboxylate group, the corresponding TS (IS_SB_2) is shown in Fig. 5b. The “moving” proton is in between N1 and O9, slightly closer to the oxygen pillar atom (O9). The relative energy of the transition state IS_SB_2 (21.1 kcal/mol, Table 3) is lower than that of IS_SB_1 reflecting the ability of the protonated terminal amino group to participate in multiple H-bonds benefiting an IS ⇔ SB transition. On the product side of the minimum energy path of this transition we found species IS_C lying at 4.0 kcal/mol relative energy (see Fig. 2c and Table 1).

Eventually, many other IS ⇔ SB transitions are possible at larger energies. One can conclude, however, that mobilization of the acidic proton of the aspartic acid side-chain requires much more energy than

Table 3
Calculated total energies (E_{tot}, Hartree), relative energies (E_{rel}, kcal/mol), characteristic torsion angles (τ_x, degree) and selected interatomic distances (Å) of transition structures belonging to IS ⇔ SB transitions on the PES of protonated RD-NH_2

TS	E_{tot}	E_{rel}	τ_1	τ_2	τ_3	Selected interatomic distances (Å)
IS_SB_1	−1023.045419	27.4	139.8	28.9	131.4	$r_{O10\cdots N7}$=2.728, $r_{N6\cdots O9}$=2.829, $r_{O9\cdots Hac}$=2.086, $r_{O2\cdots Hac}$=1.786
IS_SB_2	−1023.055505	21.1	54.1	123.9	175.0	$r_{N7\cdots O10}$=2.742, $r_{N6\cdots O2}$=2.851, $r_{N1\cdots O9}$=2.484, $r_{N1\cdots O4}$=3.024

For the numbering of the atoms, see Fig. 5a–b. The relative energies were calculated with respect to the total energy of the most stable species on the RD-NH_2 PES. Torsion angles τ_1, τ_2, and τ_3 correspond to the N1-$C^{\alpha R}$-C^{amide1}-N3, C^{amide1}-N3-$C^{\alpha D}$-C^{amide2}, and N3-$C^{\alpha D}$-C^{amide2}-N5 parameters, respectively.

mobilization of the proton added to peptides lacking any basic residues. Also, in the examples described above, the IS sides of the IS ⇔ SB transitions are at much lower energies than the SB ones. This indicates that these transitions are much faster in the IS ⇐ SB than in the IS ⇒ SB direction. As a summary we can state that while formation of SB species is energetically possible during ion activation in the mass spectrometer, the IS ⇒ SB transition is very probably kinetically controlled and only a small fraction of protonated RD-NH_2 species is present as an SB structure. Based on the analysis of the various SB species one can state that *if* the IS ⇔ SB transition is made, the mobile proton on the backbone of RD-NH_2 can "visit" various protonation sites and can induce non-selective fragmentation (see below).

4.3. Mechanisms of the selective cleavage at aspartic acid residues

Total and relative energies, and selected geometry parameters of species that may participate in various pathways of NH_3 loss of protonated RD-NH_2 are collected in Tables 4 and 5, respectively. We discuss four pathways (Scheme 1), two of which have been proposed in the literature [1,4] but two new routes were determined by our theoretical calculations.

The first step of the Yu mechanism [1] (Path A, Scheme 1, compiled for RD-NH_2) is the transfer of the acidic proton of the D side-chain to the nitrogen of the terminal amide bond. In the next step, the N-protonated terminal amide bond would be cleaved to result in a charged cyclic anhydride and neutral NH_3. The only candidate obtained in our search of the PES of protonated RD-NH_2 for the SB intermedier of the Yu mechanism is species SB_N5 (Fig. 3f). As we described above, this species is stabilized by strong hydrogen bonds formed between the terminal amino (N1) and amide terminal NH_3^+-CO (N5); the amide terminal NH_3^+-CO (N5) and COO^- (O9); and the protonated guanidine (N6 and N7) and COO^- (O9 and O10) groups, respectively. These strong intramolecular hydrogen bonds result in a very compact structure, the distortion of which requires substantial energy.

Table 4
Energetical details of the pathways leading to loss of ammonia from protonated RD-NH_2 via the four-center-one-step (FCOSx, Scheme 1b, Path C) and the oxazolone mechanisms (OXAZ, Scheme 1b, Path D)

Pathway	RC		TS		PRC		FP	
	Species	E_{rel}	E_{tot}	E_{rel}	E_{tot}	E_{rel}	E_{tot}	E_{rel}
FCOS_A	IS_A	0.6	−1022.999592	56.2	−1023.064869	15.2	−966.484496	23.6
FCOS_B	IS_G	11.1	−1023.007404	51.3	−1023.042643	29.1	−966.481283	25.6
FCOS_C	IS_H	14.8	−1023.005936	52.2	−1023.055529	21.1	−966.477063	28.3
FCOS_D	IS_F	7.9	−1023.025485	39.9	−1023.050947	23.9	−966.470673	32.3
OXAZ	SB_N5	32.3	−1023.020007	43.3	−1023.021673	42.3	−966.453686	42.9

Total energies (E_{tot}, Hartree), relative energies (E_{rel}, kcal/mol) are presented for the reactive configurations (RC), the transition structures (TS), the post-reaction complexes (PRC), and the separated final products (FP). The relative energies were calculated with respect to the total energy of the most stable species on the RD-NH_2 PES.

Table 5
Selected geometry parameters (characteristic torsion angles (τ_x, degree) and selected interatomic distances (Å)) for the transition structures of the FCOS_X and OXAZ pathways of protonated RD-NH_2

Pathway	τ_1	τ_2	τ_3	Selected interatomic distances (Å)
FCOS_A	−19.1	74.1	133.9	$r_{N3\cdots N1} = 2.655$, $r_{N6\cdots O2} = 2.711$, $r_{N7\cdots O4} = 2.989$, $r_{O9\cdots Camide} = 2.134$, $r_{Term.amide} = 1.533$
FCOS_B	20.0	−45.5	128.5	$r_{N3\cdots N1} = 2.656$, $r_{N6\cdots O2} = 2.782$, $r_{N7\cdots O4} = 2.969$, $r_{O9\cdots Camide} = 2.245$, $r_{Term.amide} = 1.514$
FCOS_C	−18.0	−112.6	−165.4	$r_{N8\cdots O2} = 2.740$, $r_{N1\cdots N3} = 2.645$, $r_{O9\cdots Camide} = 2.216$, $r_{Term.amide} = 1.565$
FCOS_D	−38.6	161.0	179.7	$r_{N3\cdots N1} = 2.721$, $r_{N6\cdots O10} = 2.795$, $r_{N7\cdots O9} = 2.988$, $r_{O10\cdots Camide} = 2.025$, $r_{Term.amide} = 1.630$
OXAZ	−177.2	0.0	−88.7	$r_{N5\cdots O9} = 2.909$, $r_{N6\cdots O9} = 2.808$, $r_{N7\cdots O10} = 2.766$, $r_{O2\cdots C(O4)} = 1.591$, $r_{N5\cdots C(O4)} = 2.233$

For the numbering of the atoms, see Figs. A–d. Torsion angles τ_1, τ_2, and τ_3 correspond to the N1-$C^{\alpha R}$-C^{amide1}-N3, C^{amide1}-N3-$C^{\alpha D}$-C^{amide2}, and N3-$C^{\alpha D}$-C^{amide2}-N5 parameters, respectively.

Although it was not noted explicitly in the original paper [1], the cleavage of the protonated (terminal) amide bond in the Yu mechanism should coincide with the attack of the COO^- group on the carbon center of the terminal amide bond to be cleaved in order to form the cyclic anhydride product ion. We tried to model this step by shortening the distance of O9 and the carbon center of the terminal amide bond starting from the stationary structure SB_N5 (Fig. 3f). During these calculations we fixed the O9–C_{amide} distance at various values and optimized all the other geometrical parameters. The calculations show that a large amount of energy is needed to distort SB_N5 to force the COO^- moiety close to the carbon of the protonated amide bond. Meanwhile, the N5–C bond distance does not lengthen very much. Relaxation (full geometry optimization) of the geometries obtained from the constrained optimization lead to SB_N5 in all cases even from that geometry resulting in partial geometry optimization of SB_N5 with the O9–C distance constrained at 1.6 Å. From these calculations we conclude that the Yu mechanism does not play a role in the ammonia loss reaction from the terminal amide of protonated RD-NH_2. This is mainly attributed to the facts that SB_N5 has a highly packed structure stabilized by strong H-bonds which would be seriously disturbed by a nucleophilic attack of COO^- on the carbon center of the protonated amide bond, and COO^- is not a strong nucleophile.

The mechanism (Scheme 1a, Path B compiled for protonated RD-NH_2) proposed by Price et al. [4] is quite similar to that proposed by Yu et al. [1] As mentioned above, the main difference between the two schemes is that the Price mechanism takes into account the possible stabilizing effect of a nearby protonated guadinie group on the stability of the SB formed by the carboxylate group and the protonated amide nitrogen. This stabilizing effect is clearly present in species SB_N5 in a form of strong hydrogen bonds. Indeed, SB_N5 is the best described if we consider it as a [protonated guanidine$^+$]$\cdots$[COO^-]$\cdots$[NH_3^+] SB. According to Price et al. [4], the second step of the complex mechanism would be simple cleavage of the protonated amide bond. BIRD data obtained for the +11 ion of ubiqutin show a very high frequency factor that indicates an entropically favored process like a direct bond cleavage [4]. However, simple cleavage of the protonated amide bond would leave an extremely reactive –CO^+ group in the product ion of this pathway (Scheme 1a, Path B). One possibility for the fate of this very reactive positive acyllium center is stabilization by a nuclephilic attack of the nearby carboxylate group of the D side-chain. This stabilization would lead back to a modified version of the Yu mechanism [1], where cleavage of the protonated amide bond occurs first and the second step is the nucleophilic attack of the carboxylate group in the remaining acyllium center. To test this hypothesis for the case of protonated RD-NH_2 we carried out constrained optimizations on SB_N5 by fixing the N5–C distances at various values while relaxing all the other geometrical parameters. These calculations show that at slight distortions of the N5–C distance the overall structure of SB_N5 does not change too much. However, at larger N5–C distances the structure of this ion undergoes a substantial change, namely a nucleophilic

attack of the *oxygen of the R–D amide bond* (O2) occurs on the carbon of the amide bond to be cleaved. On the other hand, nucleophilic attack of the carboxylate group *does not* take place. Therefore, we suggest that the mechanism proposed by Price et al. [4] for the cleavage of the amide bond adjacent to the D58 residue of the +11 ubiquitin ion, i.e., the formation of a SB intermedier and direct bond cleavage in the second step, does not play a role in the ammonia loss reaction of protonated RD-NH_2.

Contrary to the pathways proposed by Yu et al. [1] and Price et al. [4], both of which, more or less, involve a SB intermedier, we propose a mechanism that starts from IS structures. It should be noted again that it is not likely that SB-type species take part in the mechanism of *selective* cleavage at aspartic acid residues in peptides containing both acidic and basic amino acids. Whenever a SB is formed the byproduct mobile proton can very probably "visit" various backbone protonation sites and can induce random fragmentation at the backbone amide bonds.

As was described above, the IS species contain several very flexible torsion angles. For example, the side-chain of aspartic acid can rotate rather freely whenever the carboxylic group is not involved in solvation of the protonated guanidine moiety. During its rotation the hydroxyl group can get close to the carbon center of the terminal amide bond. Thus, simultaneous ring formation and transfer of the acidic proton to the amide nitrogen can occur via a FCOS mechanism. Such a reaction (Scheme 1b, Path C) results in formation of a cyclic anhydride and cleavage of the attacked amide bond (loss of ammonia from the amide terminus of protonated RD-NH_2).

To investigate the energetics of such a reaction we explored various IS conformers of protonated RD-NH_2. As mentioned above, free rotation of the aspartic side-chain can enhance the FCOS reaction. The attack of the hydroxyl oxygen of the carboxylate group on the amide carbon is entropically favored since the reaction results in a five-membered species. Of course, the strength of the terminal amide bond to be cleaved is also an important factor considering the energetics of the ammonia loss. As already mentioned, the interaction between the protonated guanidine and the amide groups has a profound effect on the strength of the amide bonds. On the other hand, the interaction between the protonated guanidine and the COOH groups can lead to significant weakening of the O–H bonds (i.e., increased acidity of the OH group). Although this interaction works against the free rotation of the COOH group, there may exist appropriate alignments, i.e., when the OH group is involved in a H-bond with the nitrogen of the terminal amide bond (such as shown in Fig. 2f), that are reactive configurations for the loss of ammonia via the FCOS mechanism (see, e.g., IS_F in Fig. 2f). To explore the above effects more quantitatively we calculated the stationary points of the FCOS mechanism starting from four different reactive configurations.

In species IS_B (Fig. 2b) the aspartic acid side-chain rotates quite freely since it is not involved in solvation of the protonated guanidine group. Indeed, IS_B should be considered as one of a bunch of very similar species having the same backbone characteristics. These species differ one another only in the conformational features of the aspartic acid side-chain and transform into another in a very likely fast process. Consequently, the hydroxyl oxygen of the side-chain can get close to the target carbon and initiate cleavage of the terminal amide bond as shown in Fig. 6a for the calculated TS (TS_FCOS_A). In the TS of Fig. 6a, the acidic proton is already transferred to the nitrogen of the terminal amide bond while the significantly elongated O9–C distance (2.245 Å, Table 5) indicates the formation of the anhydride ring. Not surprisingly, on the product side of the minimum energy path, we found a post-reaction complex formed by the anhydride ion and ammonia. This complex has a quite low relative energy (15.2 kcal/mol) and can dissociate without passing a barrier to form the separated final products lying at 23.6 kcal/mol relative energy (Table 4). The relative energy of TS_FCOS_A is quite high at 56.2 kcal/mol (Table 4). Such a large barrier would make the corresponding reaction extremely slow in mass spectrometers operated under low-energy collision conditions. However, entropy effects arising from the many flexible rotations and

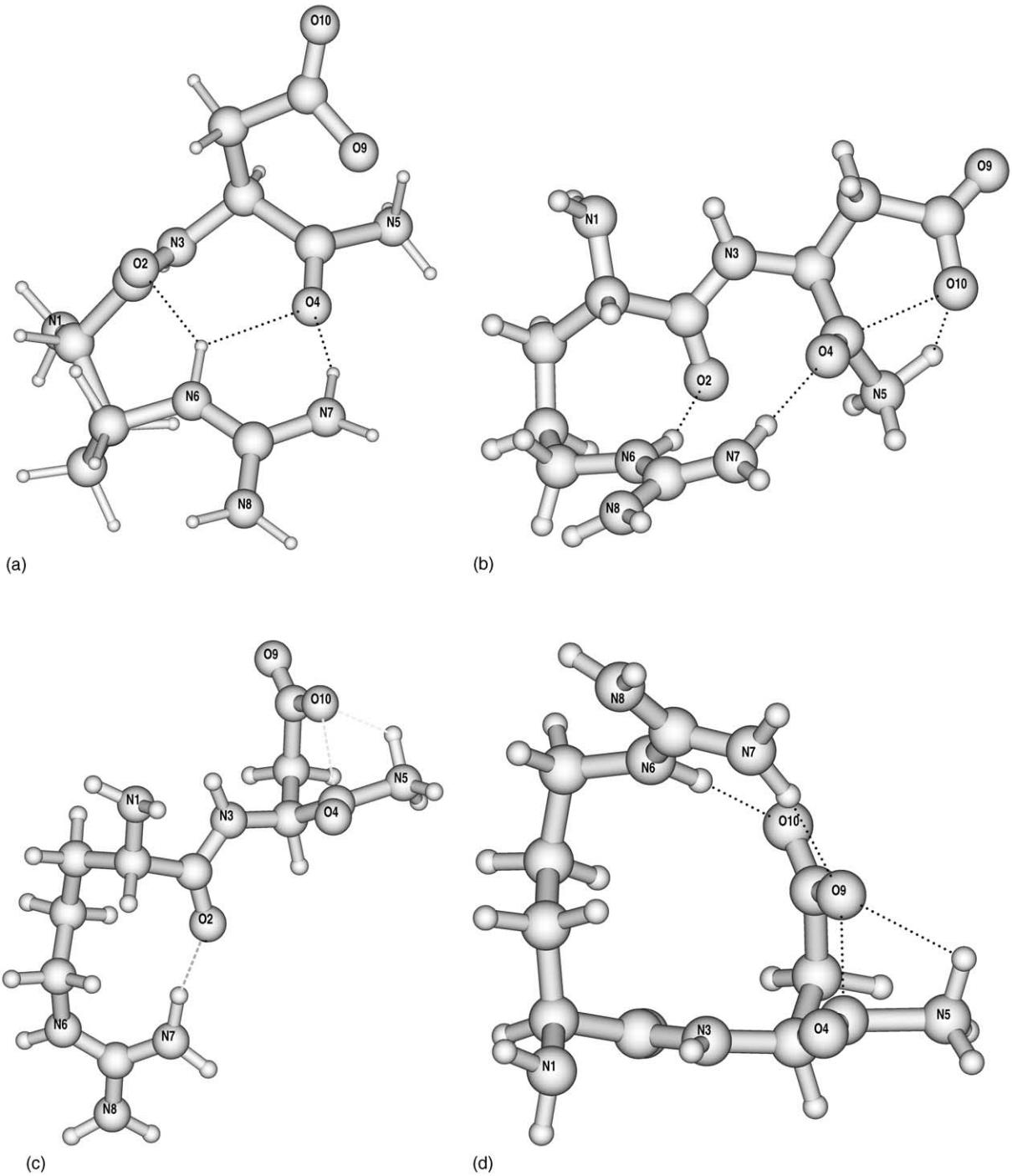

Fig. 6. Possible transition state (TS) structures for the loss of NH_3 from the terminal amide group of protonated RD-NH_2. (See text, for details.)

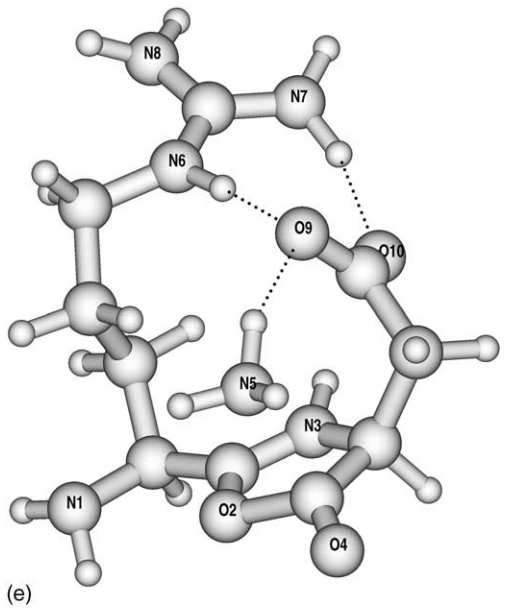

Fig. 6. (*Continued*)

the five-membered transition structure are very likely large and can result in a much smaller barrier if one considers the free energy of the entire process. Unfortunately, modeling the change of free energy during the course of this reaction is clearly out of our present capabilities.

To test other structural aspects, we determined the structural details of the NH_3 loss reaction of IS_G and IS_H (Fig. 2g and h, respectively). In IS_G the protonated guanidine group is solvated by the two amide oxygens similar to IS_B (Fig 2b) One of the main differences between IS_B and IS_G is that in IS_G, the hydroxyl oxygen (O9) is quite close to the terminal amide carbon and the OH bond is nearly parallel to the amide bond to be cleaved. Also, the terminal amide bond is longer for IS_G (1.353 Å) than for IS_B (1.341 Å). Both of these effects tend to decrease the barrier to the loss of ammonia. Consequently, the corresponding TS (TS_FCOS_B, Fig. 6b) lies at lower relative energy (51.3 kcal/mol, Table 4) than that of TS_FCOS_A (56.2 kcal/mol, Table 4).

Calculating the structural details of the ammonia loss for IS_H (Fig. 2h), we tried to model a case when the protonated arginine side-chain has no direct contact with the oxygen of the amide bond to be cleaved. As one can see in Fig. 2h, the guanidine moiety is solvated by the R–D amide oxygen (O2) causing shortening of the R–D amide bond. On the other hand, the terminal amide bond is quite long (1.361 Å). The relative energy of the TS of the ammonia-loss (TS_FCOS_C, Fig. 6c) is 52.2 kcal/mol (Table 4), similar to that of TS_FCOS_B described below. Very likely, the protonated guanidine group can still be close to the amide bond to be cleaved and can have an influence on the energetics of the fragmentation via thorough-chain interactions. To further investigate the "charge-remote" nature of the selective cleavage at D in protonated peptides containing both Arg and Asp residues, calculations on larger model compounds than RD-NH_2 are necessary.

As mentioned above, the strong interaction between the protonated guanidine and the aspartic COOH groups can weaken the OH bond significantly. If the OH bond points toward the nitrogen of the terminal amide bond (see, e.g., IS_F in Fig. 2f) in a strong H-bond interaction, one can derive another version of the FCOS mechanism. In this case, the rotation of the aspartic acid side-chain is hindered (smaller entropy effects), but the terminal amide bond is weakened considerably (1.388 Å) due to the strong O(10)-H$\cdots$N(5) H-bond. To investigate the energetics of NH_3 loss from IS_F, we calculated the corresponding TS (TS_FCOS_D, Fig. 6d). The O(9)–C_{amide} distance is 2.025 Å, the shortest amongst those calculated in FCOS TSs. Also, the terminal amide bond is long (1.630 Å) compared to those in the other FCOS TSs. Furthermore, the relative energy of TS_FCOS_D is 39.9 kcal/mol, which is lower than those of the other FCOS TSs by more than 10 kcal/mol. On the other hand, the entropy effects lowering the barrier are definitely smaller for TS_FCOS_D than those accompanying the other FCOS TSs. This is due to the strong interaction between the protonated guanidine group and the aspartic acid side-chain in IS_F ("tight" structure). For correctness, we should note, however, that, based on the available theoretical data, it is difficult to make even a qualitative prediction on

the branching ratios of the various FCOS pathways. This is mainly due to our limitations on modeling the entropy effects of these reactions.

Another mechanism (Scheme 1b, Path D) leading to loss of ammonia from protonated RD-NH_2 is initiated from the salt-bridge SB_N5 species (Fig. 3f) which was seriously explored above from the points of views of the Yu et al. [1] and Price et al. [4] mechanisms. As we proposed above, after the IS ⇔ SB transition is made, the various SB structures can very possibly transfer into each other, and therefore the presence of SB_N5 at least in a limited fraction cannot be excluded in the mass spectrometers operated under the most common ion activation conditions. As we also discussed above, protonation occurs in SB_N5 at the terminal amide nitrogen which results in an enhanced partial positive charge of the carbon of this amide bond. Such a carbon is clearly an excellent target for a nucleophilic attack. Closer look at the structure of SB_N5 (Fig. 3f) shows that the oxygen of the R–D amide bond (O2) is quite close (3.026 Å) to this partially positive carbon center. In one of our previous papers [26] we have shown that such an arrangement of the atoms (two adjacent amide bonds) of protonated *N*-formyl-glycine-amide is a reactive configuration for the ammonia loss reaction of that species. We also showed that this pathway leads to formation of a stable five-membered ring oxazolone derivative, in accordance with the available experimental results [27]. A similar reaction—initiated by the attack of O2 on the carbon of the protonated amide bond—is clearly possible for SB_N5, too. At the calculated TS (TS_OX, Fig. 6e), the five-membered oxazolone ring (OX) is nearly formed while the lengthened N5–C_{amide} bond indicates the loss of NH_3. The relative energy of TS_OX is only 43.3 kcal/mol (Table 4), just a few kcal/mol higher than that of the energetically most preferred FCOS pathway (TS_FCOS_D, 39.9 kcal/mol). On the product side of TS_OX we located an ion–molecule complex (CO_OX), which is not shown because its structure is very similar to that of TS_OX (Table 4). This complex is formed between an oxazolone-containing ion (FP_OX) and ammonia. The relative energy of this post-reaction complex is very close to that of TS_OX. This is partially due to the very weak binding of ammonia to FP_OX but instability of FP_OX also plays a role in this effect.

The energetics of the FCOS and OX pathways are compared in Fig. 7 where the relative energies of the species occurring on these pathways are plotted against the "reaction coordinate" variable. The FCOS pathways are initiated from an energetically low-lying reactive configuration and should pass

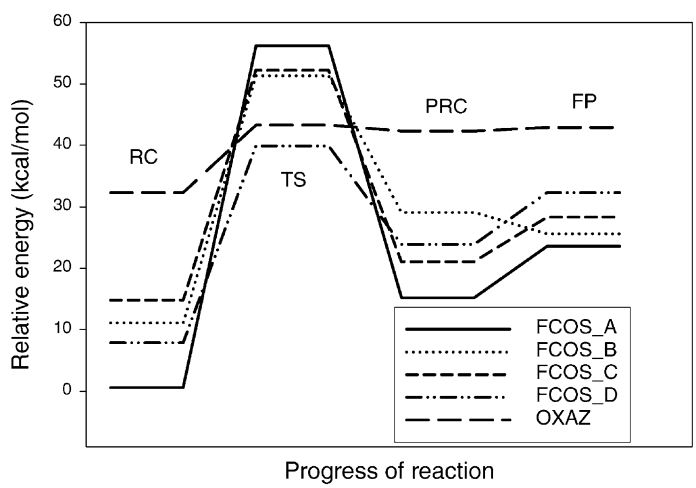

Fig. 7. Energy profiles of the "FCOS" and "OX" mechanisms.

through medium to high-energy TSs (TS_FCOS_A (56.2 kcal/mol), and TS_FCOS_D (39.9 kcal/mol)). Both the post-reaction complexes and the separated final products have much lower relative energies than those of TS_FCOS_X. It is worth noting here that the formation of the reactive configurations for the FCOS pathways requires quite a small energy. Many similar pathways are also possible from other energetically low-lying reactive configurations but these are not described and discussed here.

On the other hand, pathway OX is initiated from an energetically less preferred species SB_N5, which can be formed through various IS ⇔ SB and subsequent proton transfer reactions (see above). However, once SB_N5 is formed, the subsequent TS leading to loss of ammonia from this ion is energetically similar to TS_FCOS_D. Since we did not carry out very detailed calculations on the possible IS ⇔ IS, IS ⇔ SB, and SB ⇔ SB transitions, and cannot predict entropy changes during the FCOS pathways, we cannot unambiguously decide in what extent the OX and FCOS pathways contribute to the loss of ammonia from protonated RD-NH_2.

As an attempt to answer this question, we refer back to the MS/MS spectra of protonated RD-NH_2. As we showed above, the $[MH\text{-}NH_3]^+$ ions FP_OX and FP_FCOS are isomers and, therefore, should exhibit different fragmentation patterns. Indeed, FP_OX is an oxazolone derivative (Scheme 1b, Path D) and is expected to fragment by loss of CO. On the other hand, FP_FCOS contains a cyclic five-membered anhydride that can decompose by joint losses of CO and CO_2. The MS/MS/MS (MS^3) spectrum obtained for $[MH\text{-}NH_3]^+$ (Fig. 1b) does not show ions associated with direct CO and/or subsequent CO and CO_2 losses from $[MH\text{-}NH_3]^+$. (As discussed above losses of ammonia from the N-terminal amide group and the arginine side-chain are the most preferred fragmentation pathways of protonated RD-NH_2.) Instead, the most dominant ion corresponds to the loss of an extra NH_3 (*m/z* 255), from which subsequent CO (*m/z* 227) and CO_2 (*m/z* 183) losses are observed (the MS^4 spectrum on $[MH\text{-}2NH_3]^+$ is not shown). Because of the presence of *m/z* 183 in the fragmentation spectrum of $[MH\text{-}2NH_3]^+$, an anhydride structure corresponding to the FCOS mechanisms can be rationalized. On the other hand, the presence of *m/z* 227 (CO loss) suggests that the oxazolone pathway (OX) cannot be excluded, either. Thus, we can conclude that the NH_3 loss from the terminal amide group of protonated RD-NH_2 takes place through both the FCOS and OX pathways. It is interesting to note here that in the fragmentation spectrum of $[MH\text{-}2NH_3]^+$ generated by subsequent losses of NH_3 from protonated RGD-NH_2, no ion corresponding to the loss of CO is observed. The most intense fragment ion corresponds to the loss of 72 (presumably related to the loss of O=C–O–C=O from the anhydrate structure) [28].

5. Conclusions

A detailed theoretical and MS/MS investigation has been carried out on protonated RD-NH_2, which is one of the simplest model for peptides containing both basic (R) and acidic (D) amino acids. Our computational and experimental results clearly suggest that IS species are more stable than ions with a SB formation. In the IS structures, the acidic proton of the Asp side-chain is not mobilized and can generate selective cleavages, including the loss of NH_3 from the terminal amide group. In the SB structures, the ionizing proton is mobile and can initiate non-selective cleavages. Our calculations also imply that mobilization of the acidic proton of the aspartic acid side-chain (a possible IS ⇔ SB transition) requires much larger energies than mobilization of the proton added to peptides lacking any basic residues. The theoretical results indicate that the loss of ammonia from the terminal amide group of protonated RD-NH_2 can occur via two main different pathways. The “OX” pathway includes an IS ⇔ SB transition at the first step which results in a mobile proton on the backbone of RD-NH_2. Ammonia loss from species protonated at the nitrogen of the terminal amide bond can take place in the second step via formation of an ion including an oxazolone ring. Since the proton transferred to the backbone of the dipeptide is very likely mobile, the OX pathway

cannot be considered "selective." On the other hand, the FCOS pathways lead to the loss of ammonia via a selective mechanism. These pathways are initiated from energetically low-lying IS structures and do not involve any SB intermediers. Note that formation of ammonia via most of the FCOS_X pathways is entropically highly favored. The experimental MS/MS results (especially those obtained for the fragmentation of $[MH\text{-}2NH_3]^+$) support both the OX and FCOS mechanisms. This indicates that some mechanistic information on the cleavage of amide bonds adjacent to Asp (D) acid residues can be derived even from this very simple model. On the other hand, the complexity of such a simple system (i.e., different protonated structures and transition states for a particular fragmentation process) should warn us to avoid suggesting oversimplified and exclusive mechanisms for selective cleavages in larger protonated peptides.

From another aspect, the results of theoretical calculations for model peptides should also be considered carefully. For example, not all the theoretically (energetically) feasible pathways are necessarily operative in tandem MS experiments. This can be attributed, for example, to the limitations of calculations to quantitatively predict the "entropy factor." Regarding our current model, it is obvious that protonated RD-NH_2 has its own limitations in making fully generalized statements for selective fragmentation pathways at aspartic acid residues in arginine containing peptides. This peptide is just too small so that the close proximity of the Arg and Asp acid side-chains can generate several theoretical (and/or real) fragmentation pathways that are not necessarily applicable for larger peptides. According to the calculations, the ammonia loss from the amide terminus of protonated RD-NH_2 cannot be considered fully "selective" (see, e.g., the oxazolone (OX) pathway as an alternative fragmentation channel to the "FCOS" mechanisms). Thus, to model selective cleavages at Asp acid residues in larger Arg containing peptides, it will be desirable to use larger model peptides, e.g., in which the leaving group is not ammonia but an amino acid and/or in which the Asp and Arg are not neighboring residues. Tandem MS measurements and theoretical calculations on larger model peptides, such as RGD-NH_2 and RDGDR-OH, are in progress in our laboratories.

Acknowledgements

The authors are grateful to the reviewers and Vicki H. Wysocki for their useful comments.

References

[1] W. Yu, J.E. Wath, M.C. Huberty, S.A. Martin, Anal. Chem. 65 (1993) 3015.
[2] R. Bakhtiar, Q. Wu, S.A. Hofsradler, S.A. Smith, Biol. Mass Spectrom. 65 (1994) 707.
[3] J. Quin, B.T. Chait, J. Am. Chem. Soc. 117 (1995) 5411.
[4] W.D. Price, P.D. Schnier, R.A. Jockush, E.R. Williams, J. Am. Chem. Soc. 118 (1996) 10640.
[5] G. Tsaprailis, H. Nair, Á. Somogyi, V.H. Wysocki, W. Zhong, J.H. Futrell, S.G. Summerfield, S.J. Gaskell, J. Am. Chem. Soc. 121 (1999) 5142.
[6] G. Tsaprailis, Á. Somogyi, E.N. Nikolaev, V.H. Wysocki, Int. J. Mass Spectrom. 196 (2000) 467.
[7] C. Gu, G. Tsaprailis, L. Breci, V.H. Wysocki, Anal. Chem. 72 (2000) 5804.
[8] H. Nair, Á. Somogyi, V.H. Wysocki, J. Mass Spectrom. 31 (1996) 1141.
[9] A.L. McCormack, Á. Somogyi, A.R. Dongré, V.H. Wysocki, Anal. Chem. 65 (1993) 2859.
[10] Á. Somogyi, V.H. Wysocki, I. Mayer, J. Am. Soc. Mass Spectrom. 5 (1994) 704.
[11] J.L. Jones, A.R. Dongré, Á. Somogyi, V.H. Wysocki, J. Am. Chem. Soc. 116 (1994) 8368.
[12] A.R. Dongré, Á. Somogyi, V.H. Wysocki, J. Mass Spectrom. 31 (1996) 339.
[13] A.R. Dongré, J.L. Jones, Á. Somogyi, V.H. Wysocki, J. Am. Chem. Soc. 118 (1996) 8365.
[14] I.P. Csonka, B. Paizs, Gy. Lenday, S. Suhai, Rapid Commun. Mass Spectrom. 14 (2000) 417.
[15] B. Paizs, I. P Csonka, Gy. Lendvay, S. Suhai, Rapid Commun. Mass Spectrom. 15 (2001) 637.
[16] H. Nair, V.H. Wysocki, Int. J. Mass Spectrom. Ion Processes 174 (1998) 95.
[17] C. Gu, A. Somogyi, V.H. Wysocki, K.F. Medzihradszky, Analytica Chimica Acta 397 (1999) 247.
[18] Program Package TurboSEQUEST, for detailed and updated information, see, J. Eng, J. Yates III, www.fields.scripps.edu/sequest
[19] S.W. Lee, H.S. Kim, J.L. Beauchamp, J. Am. Chem. Soc. 120 (1998) 3188.
[20] R.R. Julian, R. Hodyss, J.L. Beauchamp, J. Am. Chem. Soc. 123 (2001) 3577.
[21] I. P. Csonka, B. Paizs, S. Suhai, Á. Somogyi, in preparation.
[22] B. Paizs, S. Suhai, in preparation.

[23] M.J. Frisch, G.W. Trucks, H.B. Schlegel, P.M.W. Gill, B.G. Johnson, M.A. RoCP, J. R. Cheeseman, T.A. Keith, G.A. Petersson, J.A. Montgomery, K. Raghavachari, M.A. Al-Laham, V.G.Zakrzewski, J.V. Ortiz, J.B. Foresman, J. Cioslowski, B.B. Stefanov, A. Nanayakkara, M. Challacombe, C.Y. Peng, P.Y. Ayala, W. Chen, M.W. Wong, J.L. Andres, E. S. Replogle, R. Gomperts, R. L. Martin, D. J. Fox, J. S. Binkley, D. J. Defrees, J. Baker, J. P. Stewart, M. Head-Gordon, C. Gonzalez, J. A. Pople, Gaussion Inc., Pittsburgh, PA, 1995.
[24] E. Kaiser, R.L. Colescott, C.D. Bossinger, P. Cook, Anal. Biochem. 34 (1970) 595.
[25] N.N. Dookeran, T. Yalcin, A.G. Harrison, J. Mass Spectrom. 31 (1996) 500.
[26] B. Paizs, G. Lendvay, K. Vékey, S. Suhai, Rapid Commun. Mass Spectrom. 13 (1999) 525.
[27] T. Yalcin, C. Khouw, I.G. Csizmadia, M.R. Peterson, A.G. Harrison, J. Am. Soc. Mass Spectrom. 6 (1995) 1165.
[28] B. Paizs, S. Suhai, Á. Somogyi, in preparation.